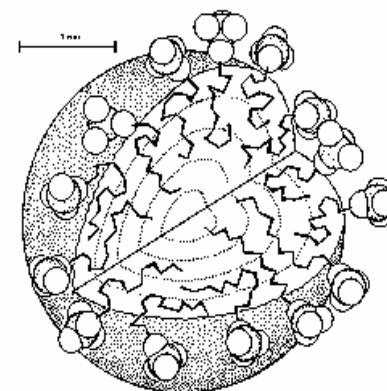


Oxford Summer School. September 2007

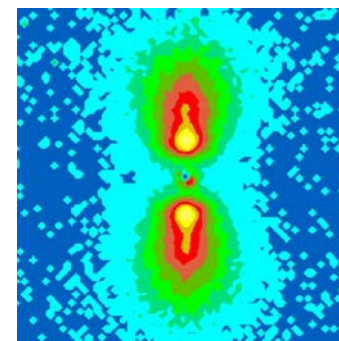
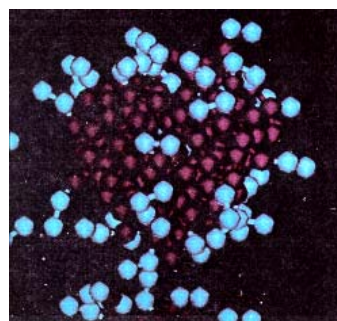
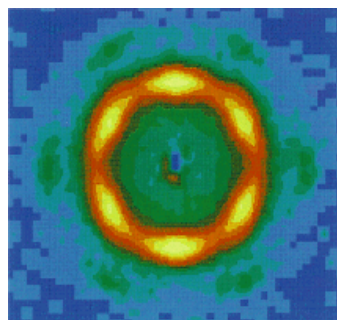
Soft Condensed Matter 2

The study of surfactant self-assembly,
and polymers in solution using
Small Angle Neutron Scattering

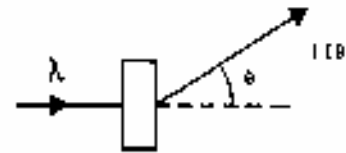
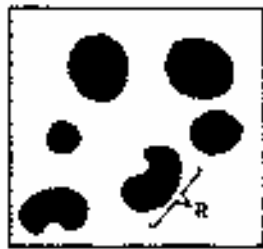


Jeff Penfold

ISIS Facility, Rutherford Appleton Lab



Small Angle Scattering



SAS is scattering in the forward direction, and is related to the scattering properties of materials at small scattering vectors, Q

Wave vector transfer Q defined as

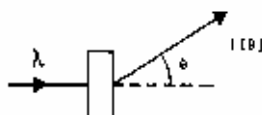
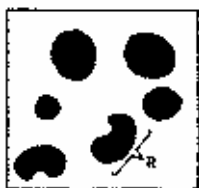
$$Q = \frac{4\pi}{\lambda} \sin \frac{\theta}{2}$$

$$\frac{d\sigma}{d\Omega} = N \left\langle \left| \sum_{i(V)} \bar{b}_i \exp(iQ \cdot R_i) \right|^2 \right\rangle_Q$$

$$Q = k_i - k_f = 2k_i \sin \frac{\theta}{2}$$

Contrast Variation

$\rho(r)$ Scattering length density

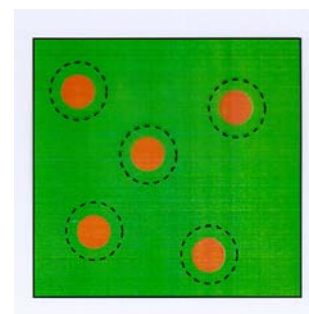
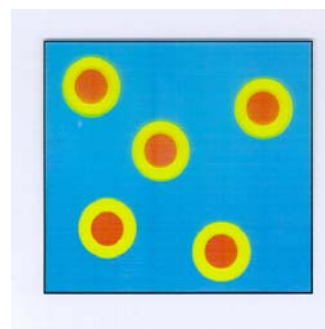
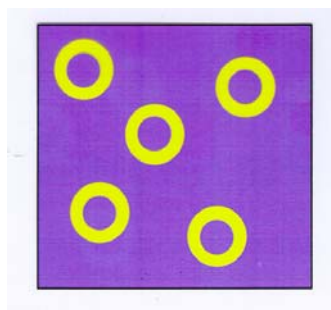


$$\rho(r)\delta v = \sum_{j(V)} b_j$$

$$\frac{d\sigma}{d\Omega} = N \left\langle \left| \int_V p(r) \exp(iQ \cdot r) dr \right|^2 \right\rangle_Q$$

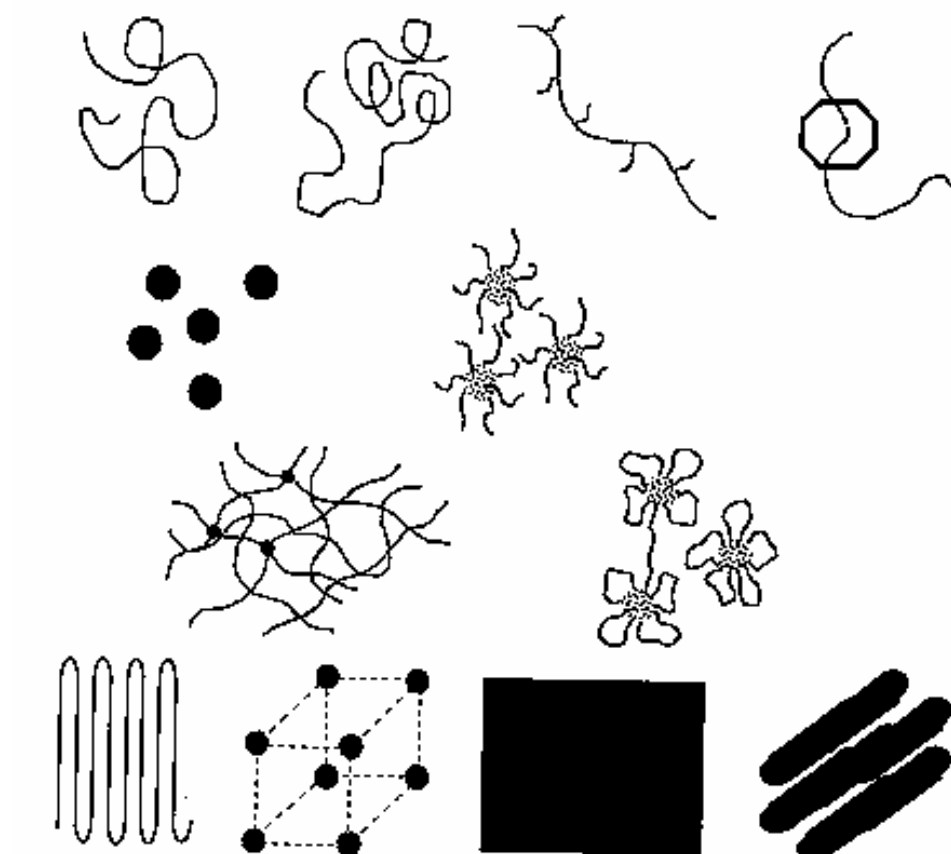
$\langle \rangle_Q$ all orientation with respect to Q

N is the number of scattering objects

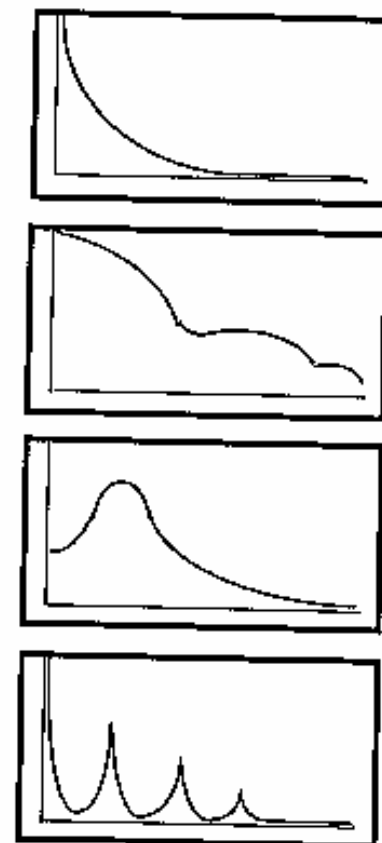


Molecule	Bulk density (g.cm ⁻³)	Molecular weight (g.mol ⁻¹)	Molar volume (Å ³)	Scattering length density (10 ¹⁰ cm ⁻²)
H ₂ O	1.0	18.015	29.915	-0.560
D ₂ O	1.112	20.0314	29.915	6.400
toluene C ₇ H ₈	0.865	92.140	176.884	0.939
C ₇ D ₈	0.9407	100.205	176.884	5.647
heptane C ₇ H ₁₆	0.684	100.20	243.267	-0.547
C ₇ D ₁₆	0.794	116.33	243.267	6.300
cyclohexane C ₆ H ₁₂	0.779	84.161	179.403	-0.278
C ₆ D ₁₂	0.891	96.258	179.406	6.685
silicon	2.329	28.0855	20.025	2.074
SiO ₂ vitreous	2.2	60.0843	45.352	3.475
SiO ₂ α quartz	2.648	“	37.679	4.183
TiO ₂	4.23	79.899	31.366	2.604
Al ₂ O ₃	3.97	101.961	42.648	5.699
poly(ethylene)-CH ₂ -	0.92	14.027	25.318	-0.329
poly(styrene) - C ₈ H ₈ -	1.05	104.151	164.71	1.412
d-poly(styrene) - C ₈ D ₈ -	1.131	112.216	164.71	6.468

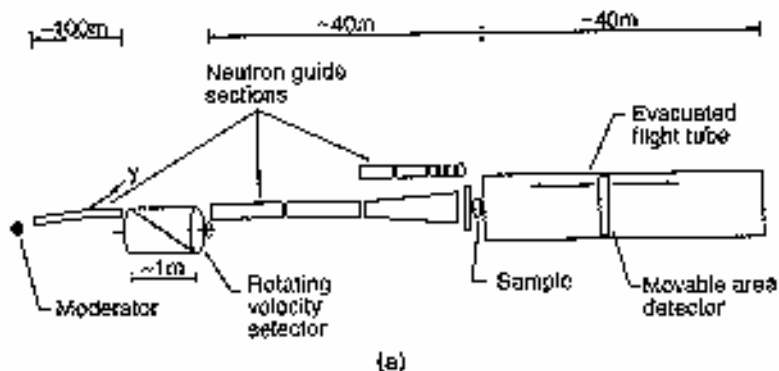
Some characteristic scattering patterns



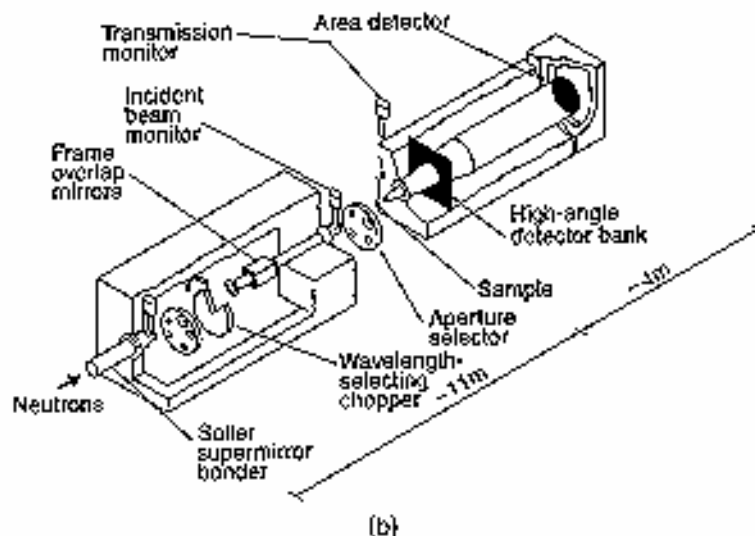
CLRC



Instrumentation



**D11/D22 (ILL)
Monochromatic**



**LOQ (ISIS)
White beam TOF**

Typical Q range 2×10^{-3} to 0.5 \AA^{-1} , Probes dimensions $(\sim 2\pi/Q) \sim 3000$ to 10 \AA

Dilute Solution : non-interacting particles

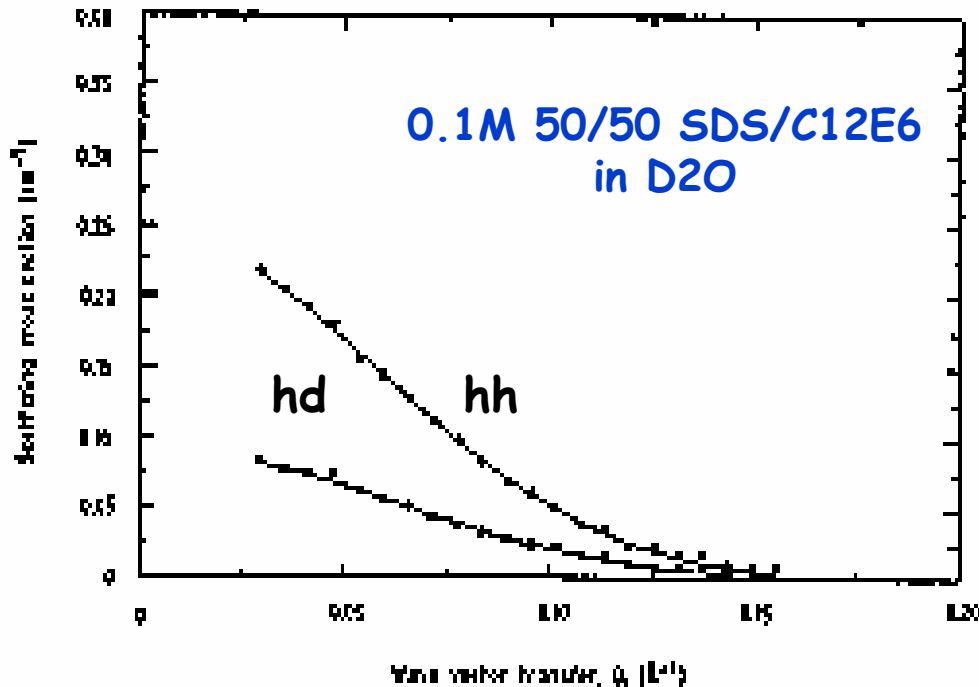
Scattering from isolated particles,
determined by particle form factor

$$\frac{d\sigma}{d\Omega} = N \langle F^2(Q) \rangle_Q$$

$$F(Q) = \int_{V_p} (\rho(r) - \rho_s) \exp(iQ \cdot r) dr$$

$$I(Q=0) = NV^2 (\rho - \rho_s)^2$$

Extrapolation to $Q=0$ determined
by scattering volume and contrast



Concentrated Solution : interacting particles

For globular interacting polydisperse particles, in the 'decoupling approx' (no correlation between position and orientation)

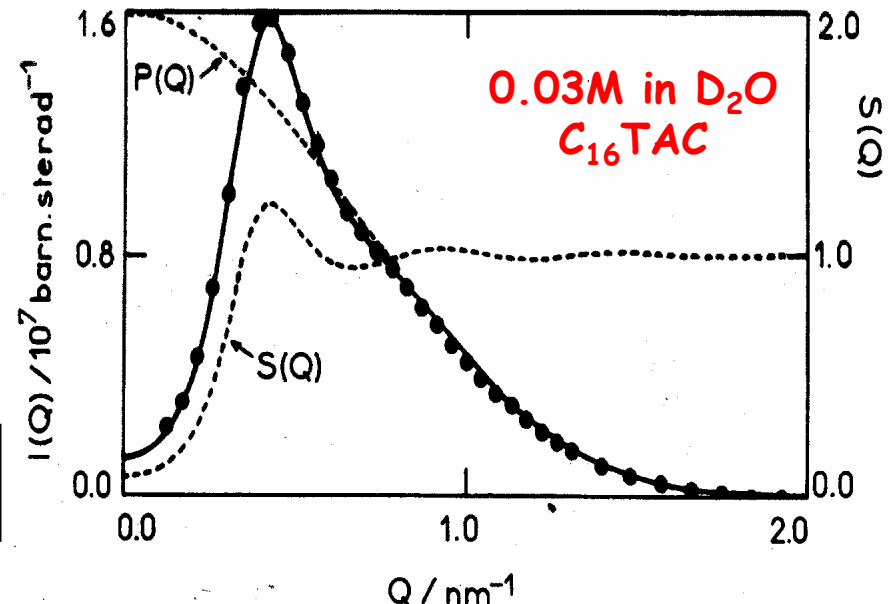
$$\frac{d\sigma}{d\Omega} = N \left[S(Q) \cdot \langle F(Q) \rangle_Q^2 + \Delta(Q) \right]$$

$$\Delta(Q) = \langle |F(Q)|^2 \rangle_Q - \langle F(Q) \rangle_Q^2$$

For monodisperse spheres

$$\frac{d\sigma}{d\Omega} = NP(Q)S(Q)$$

$$P(Q) = |F(Q)|^2$$



$S(Q)$ is the inter-particle structure factor, $\Delta(Q)$ a coherent disorder term switched on by interactions



J B Hayter, J Penfold, Colloid Polym Sci 261 (1983) 1022
M Kotlarchyck, S H Chen, J Chem Phys 79 (1983) 2461



Form Factors: Spheres and core+shell

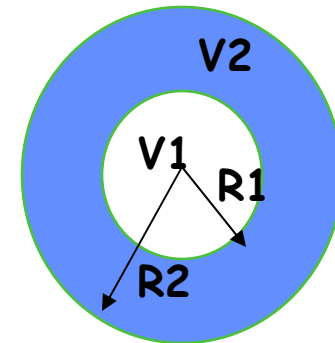
For monodisperse particles with centro-symmetry

$$\langle F^2(Q) \rangle_Q = \langle F(Q) \rangle_Q^2 = F_Q^2(Q)$$

For uniform spheres of radius R

$$F_s(Q) = V(\rho - \rho_s)F_0(QR)$$

$$V = 4\pi R^3/3$$



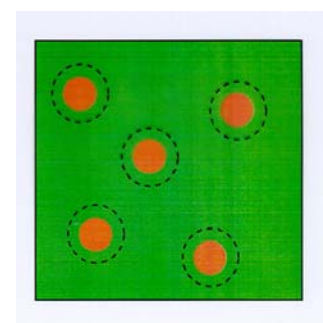
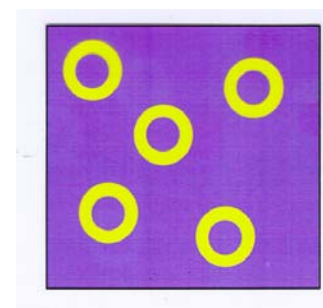
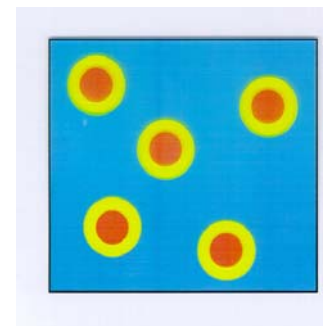
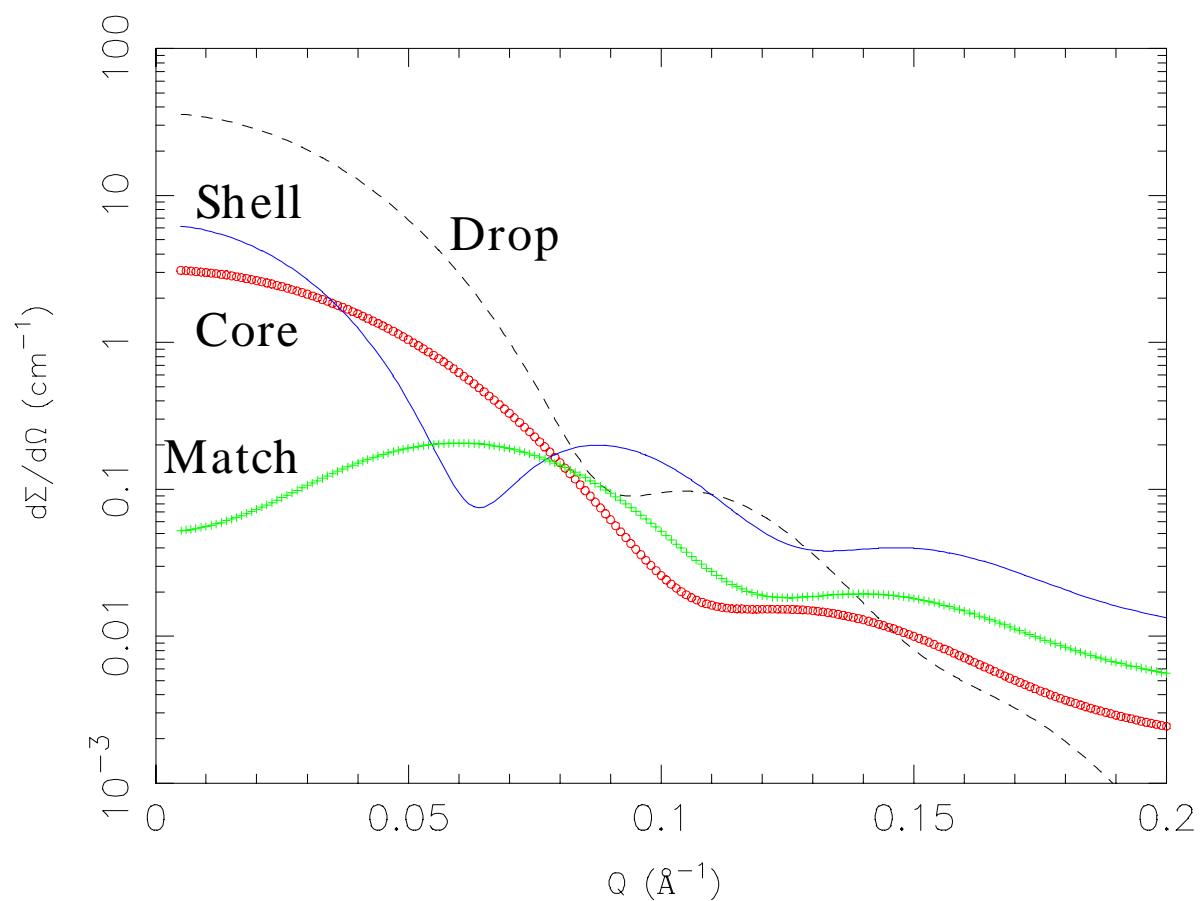
The geometrical form-factor , $F_0(QR)$, is given as,

$$F_0(QR) = 3[\sin(QR) - QR \cos(QR)]/(QR)^3 = 3j_1(QR)/(QR)$$

For m concentric spherical shells,

$$F_s(Q) = V_1(\rho_1 - \rho_2)F_0(QR_1) + V_2(\rho_2 - \rho_3)F_0(QR_2) + V_m(\rho_m - \rho_s)F_0(QR_m)$$

Drop, shell, core form-factors

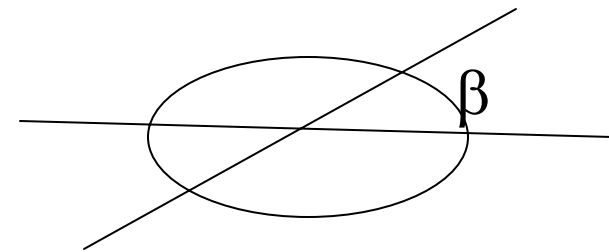


Form Factors: Ellipses and rods

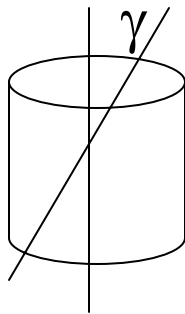
Ellipsoids

$$\langle F^2(Q) \rangle_Q = V_e^2 (\rho - \rho_s)^2 \int_0^1 F_0^2 \left\{ Qa \left[1 + (e^2 - 1)x^2 \right]^{1/2} \right\} dx$$

where $x = \cos \beta$, angle between Q and major axis of ellipsoid with axes a, a, ae



Cylinders or Rods

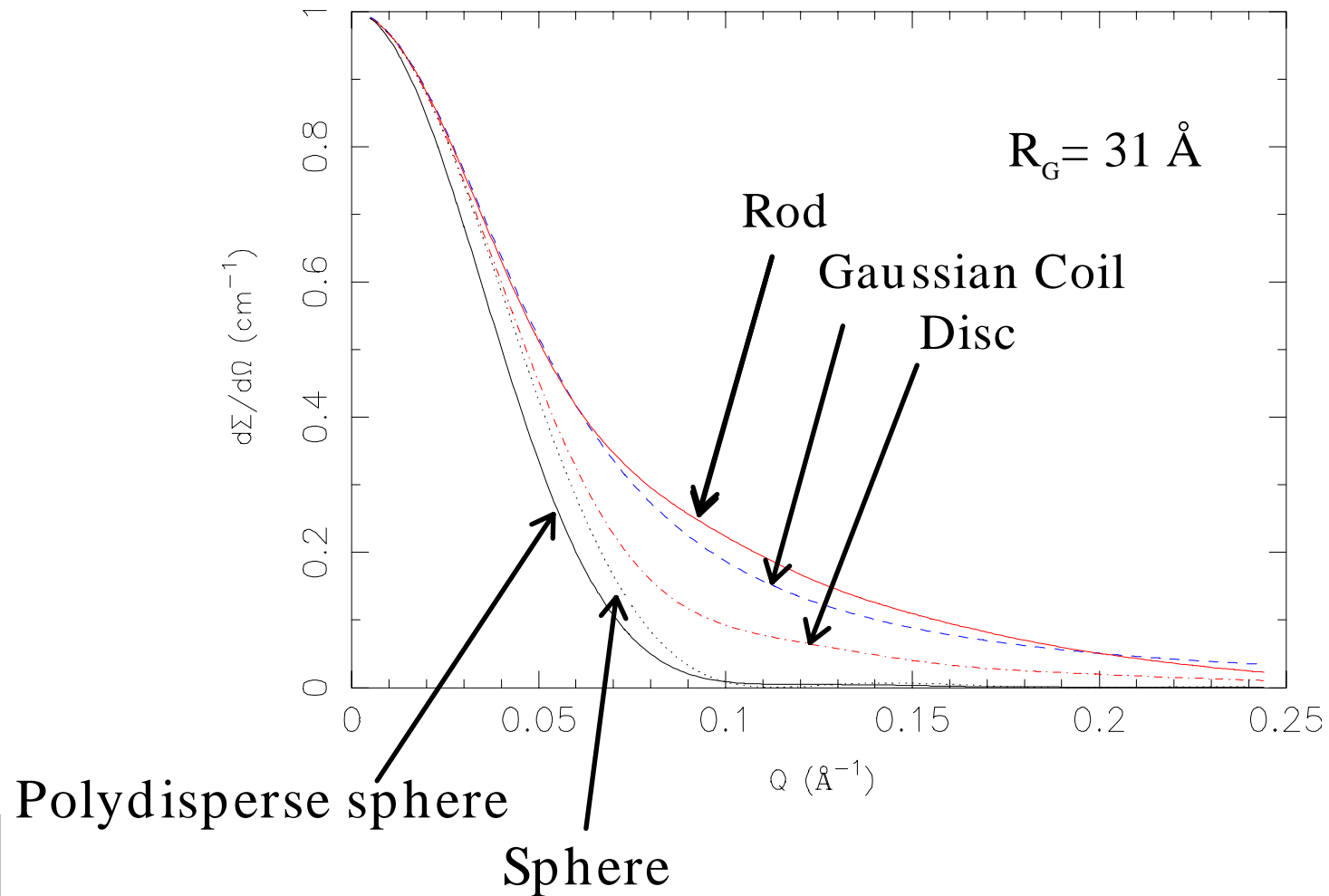


$$\langle F^2(Q) \rangle_Q = V^2 (\rho - \rho_s)^2 \int_0^{\pi/2} F^2(Q) \sin \gamma d\gamma$$

$$F(Q) = 2 j_0(Ql \cos \gamma) J_1(Qa \sin \gamma) / (Qa \sin \gamma)$$

γ is angle between Q and cylinder axis, l is rod half length, a radius, $J_1(x)$ first order Bessel function of first kind, $j_0(x) = \sin x / x$

Particle Form-factors

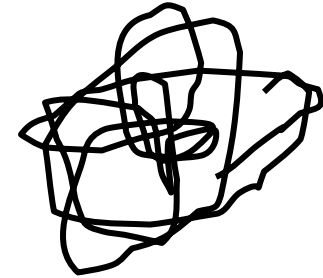


Other Form-Factors

Gaussian Coil

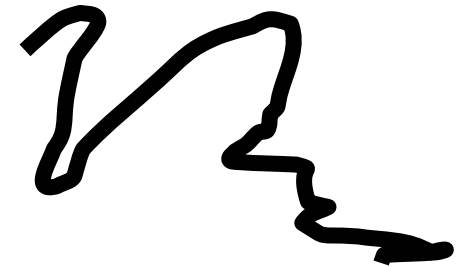
$$\frac{d\sigma}{d\Omega} = NV^2(\Delta\rho)^2 \left[\frac{2(\exp(-y^2) + y^2 - 1)}{y^4} \right]$$

$$y = QR_g$$



Kratky-Porod Worm-like Chains

$$\frac{d\sigma}{d\Omega} \approx \pi NV^2(\Delta\rho)^2 \frac{1}{QL} \exp\left(-\frac{Q^2 R_g^2}{2}\right)$$



Approximate Relationships, Limiting Laws

I(Q=0)

$$\frac{d\sigma}{d\Omega}(Q=0) \approx NV^2(\Delta\rho)^2$$

Invariant

$$\int_0^\infty Q^2 \frac{d\sigma}{d\Omega} dQ = 2\pi^2 \phi(1-\phi)\Delta\rho^2$$

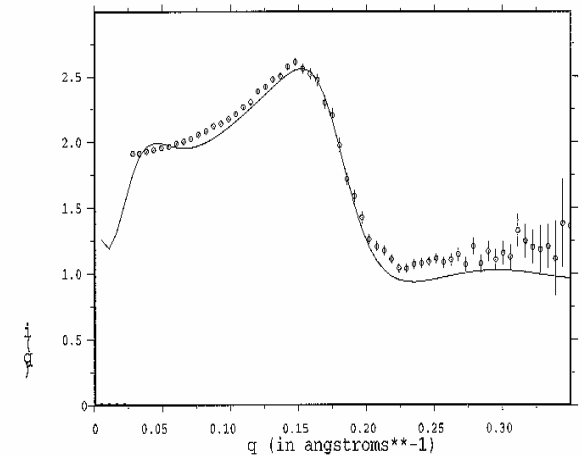
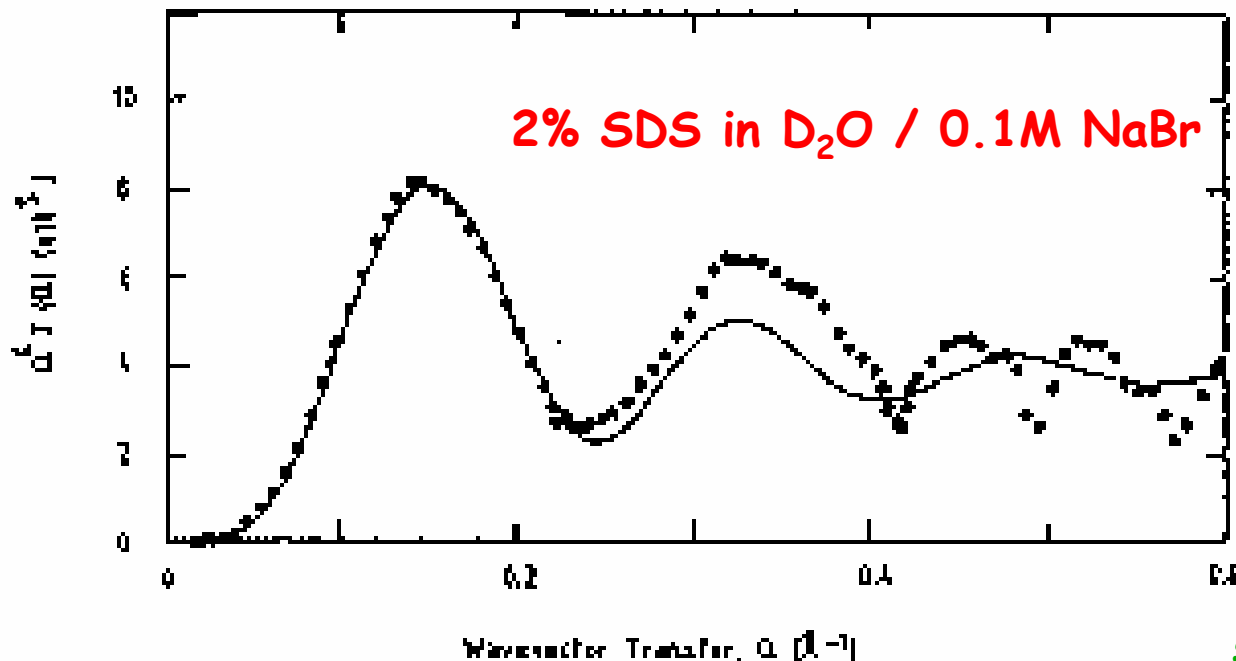
Volume fraction, $\phi=NV$, $\Delta\rho=(\rho-\rho_s)$

Provide information about total scattering volume and contrast
Important information and constraints for subsequent modelling

POROD's Law : limit at high Q

For particles with well-defined interface scattering at high Q
decays as Q^{-4} .

Extrapolation to high Q provides estimate of surface area



$$\frac{d\sigma}{d\Omega}(Q \rightarrow \infty) \approx 2\pi \frac{(\Delta\rho)^2}{Q^4} S$$

S is the surface area per unit volume of sample

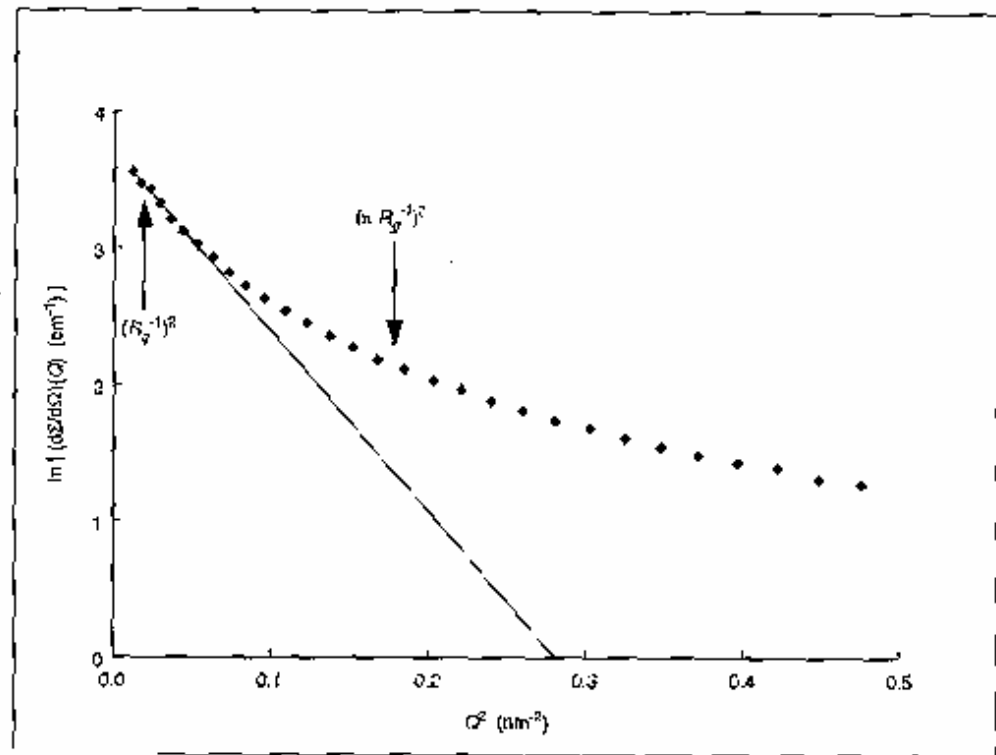


Guinier's Law

At low Q , scattering cross-section can be approximated by Guinier expansion,

Series expansion of $P(Q)$,

$$P(Q) \approx 1 - \frac{(QR)^2}{10} +$$



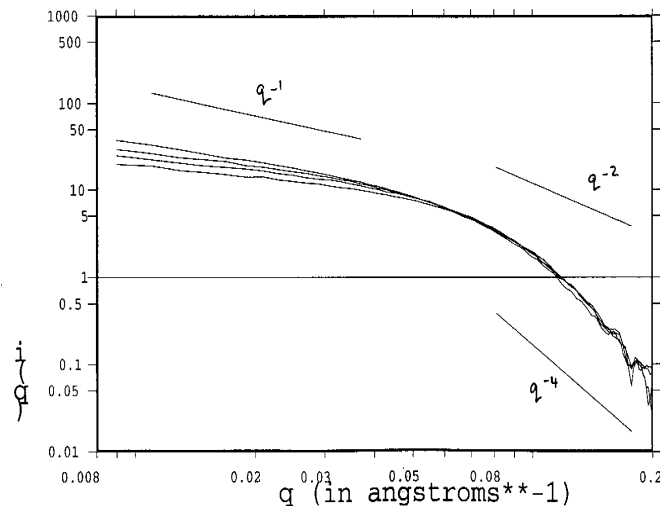
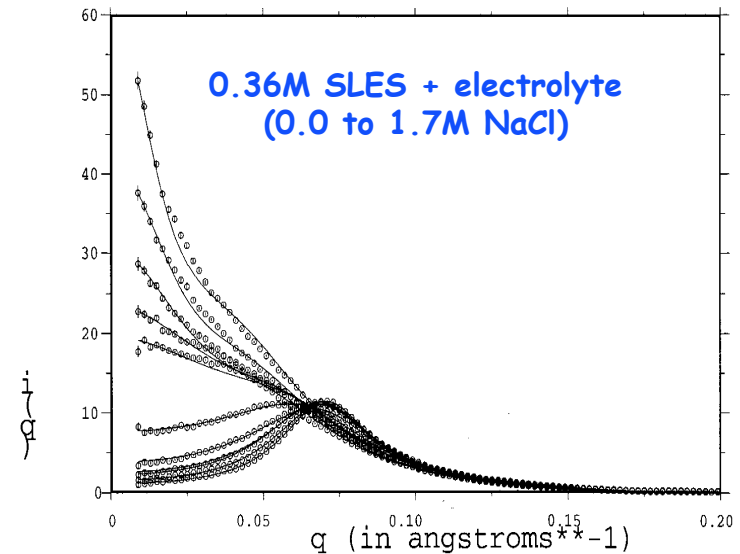
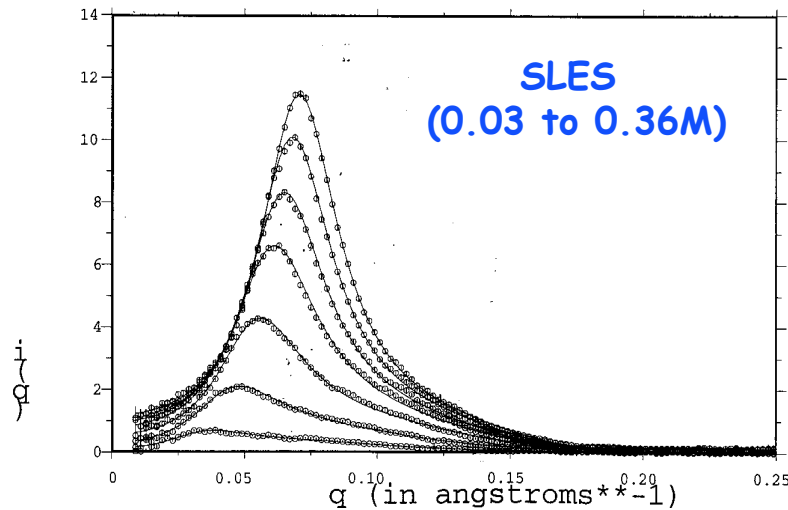
$$\frac{d\sigma}{d\Omega} \approx NV^2(\Delta\rho)^2 \exp\left(\frac{R_g^2 Q^2}{3}\right) \quad R_s^2 = \frac{5}{3} R_g^2 \quad \text{Valid for } QR_g < 1$$



Plot of Log(scattering intensity) v Q^2 is linear with slope related to R_g and intercept $NV^2(\Delta\rho)^2$



For rod-like or elongated structures



At low to intermediate Q , Q^{-1} dependence

$$Q \frac{d\sigma}{d\Omega} = \pi N V^2 (\Delta\rho)^2 \exp \left(-\frac{(QR_c)^2}{2} \right)$$

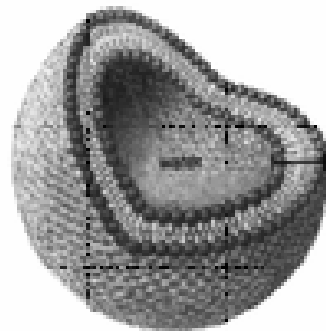
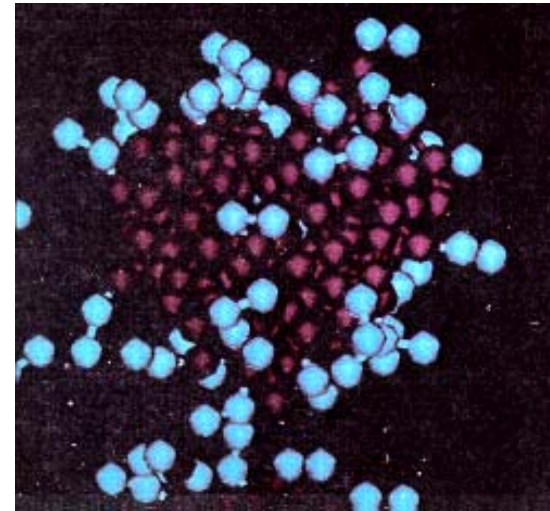
At intermediate Q , or $QR_c < 1$, a plot of $\log Q d\sigma/d\Omega$ v Q^2 will be linear, Q^{-2} Guinier regime

At high Q , Q^{-4} dependence, the scattering contains only information about the local rod cross-section

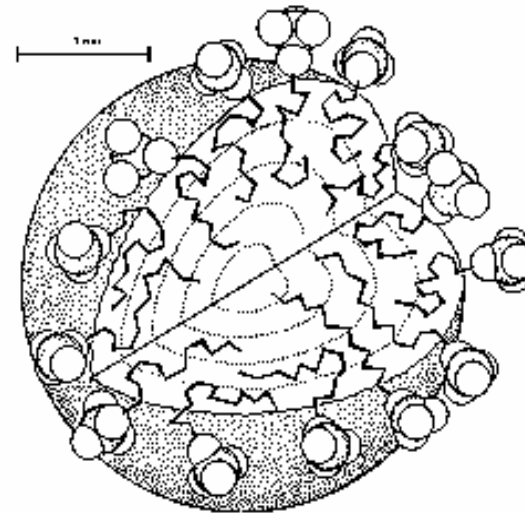
$$\frac{d\sigma}{d\Omega} \approx \frac{4\pi}{Q} \left(\frac{J_1(QR_c)}{QR_c} \right)^2$$

Self-Assembly

Surfactant micelles and meso-phases



Vesicle



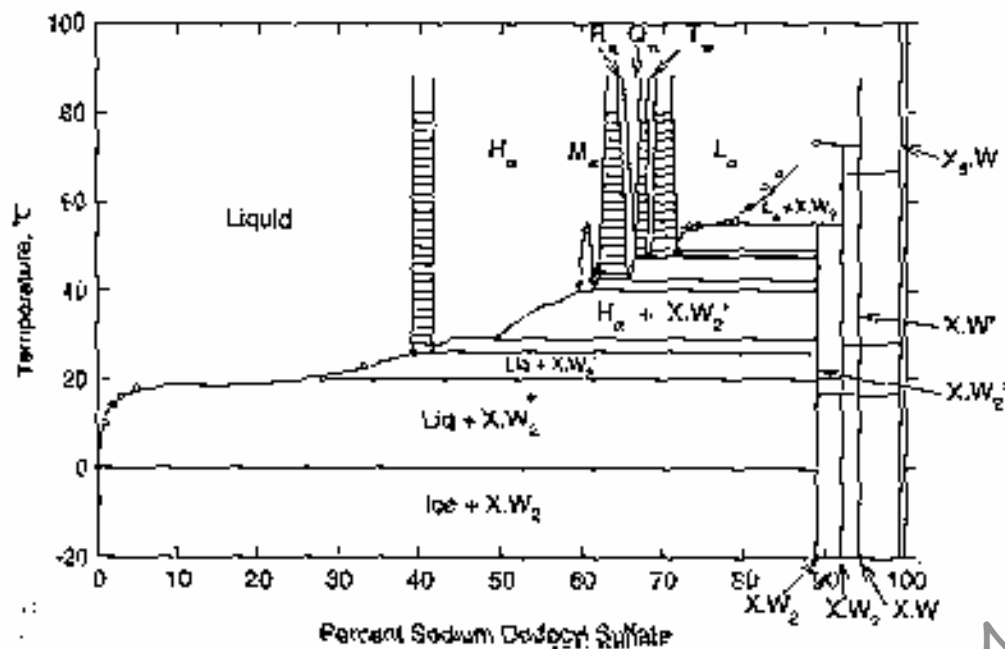
*J Penfold, Encyl of Surface and
Colloid Science (2002) Marcel Dekker, NY*

Surfactants (solution behaviour)

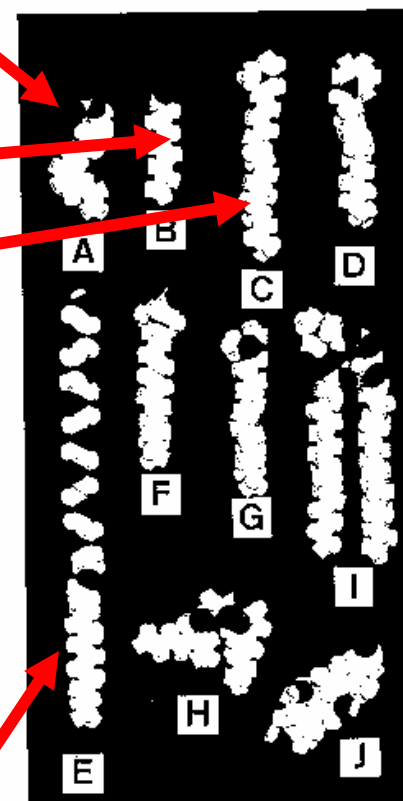
Sodium dodecyl sulphate, SDS
 $\text{CH}_3(\text{CH}_2)_{11}\text{OSO}_3^-\text{Na}^+$

Sodium Octanoate, NaO
 $\text{CH}_3(\text{CH}_2)_7\text{CO}_2^-\text{K}^+$

n-hexadecyltrimethyl ammonium bromide
 C_{16}TAB , $\text{CH}_3(\text{CH}_2)_{15}\text{N}^+(\text{CH}_3)_3\text{Br}^-$

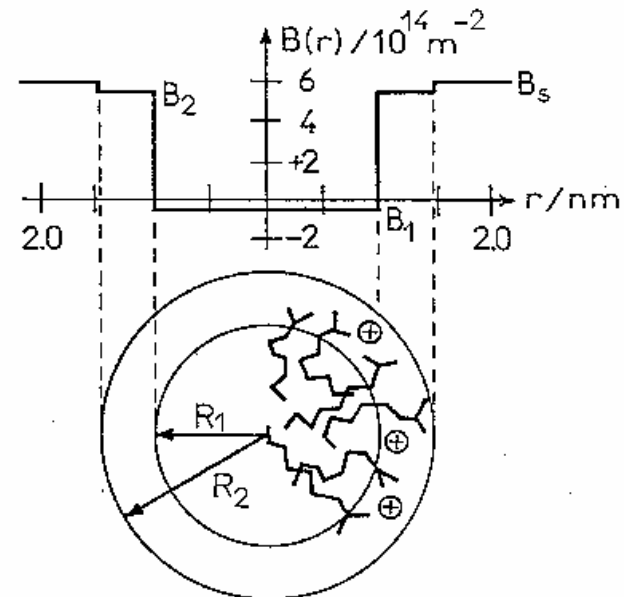
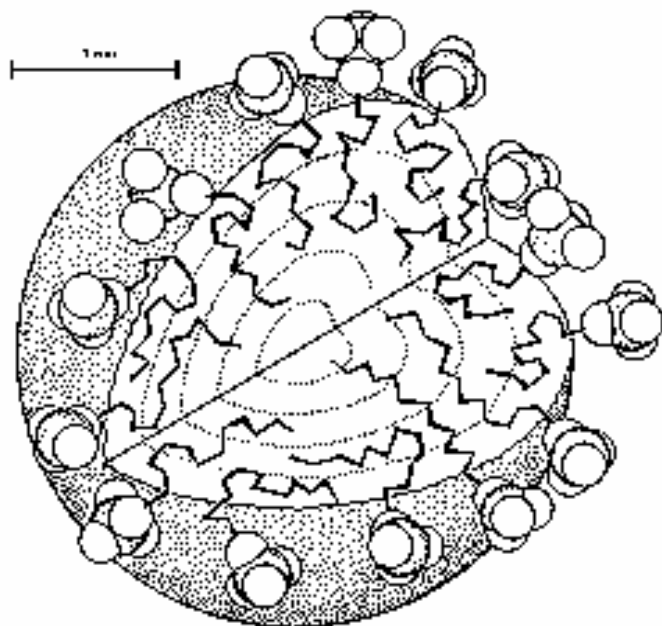


Phase diagram for SDS

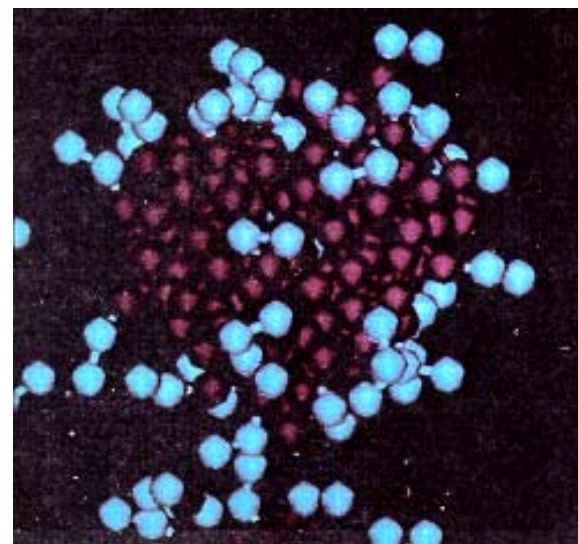


N-dodecyloctaetyleneglycol monoether
 $\text{CH}_3(\text{CH}_2)_{11}(\text{OCH}_2\text{CH}_2)_8\text{OH}$

Micelle Structure

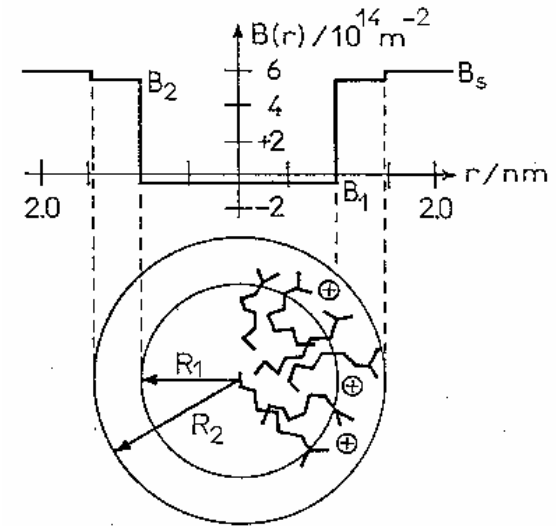
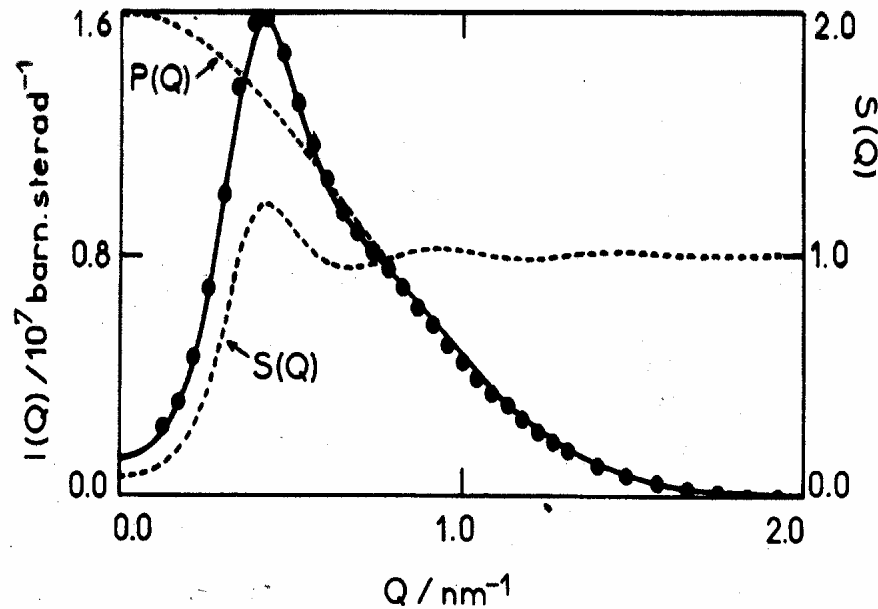


Gruen, Prog Coll Polym Sci (1985) 70 6

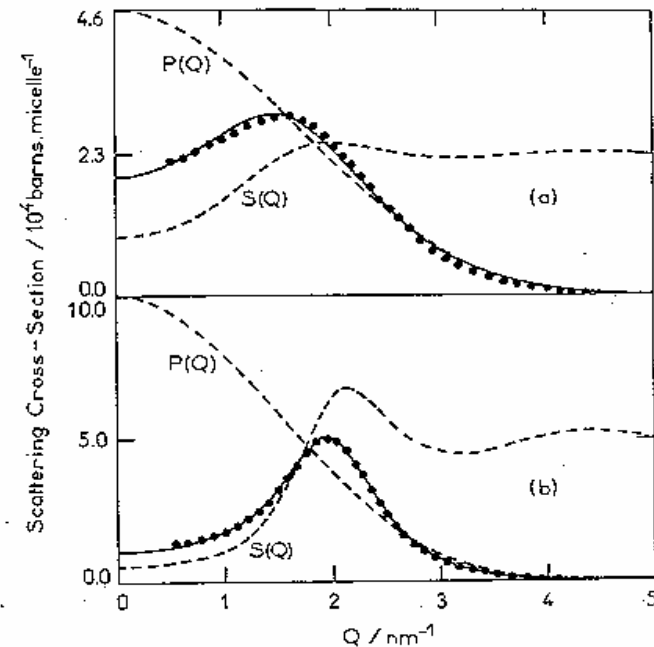


Micelle Structure

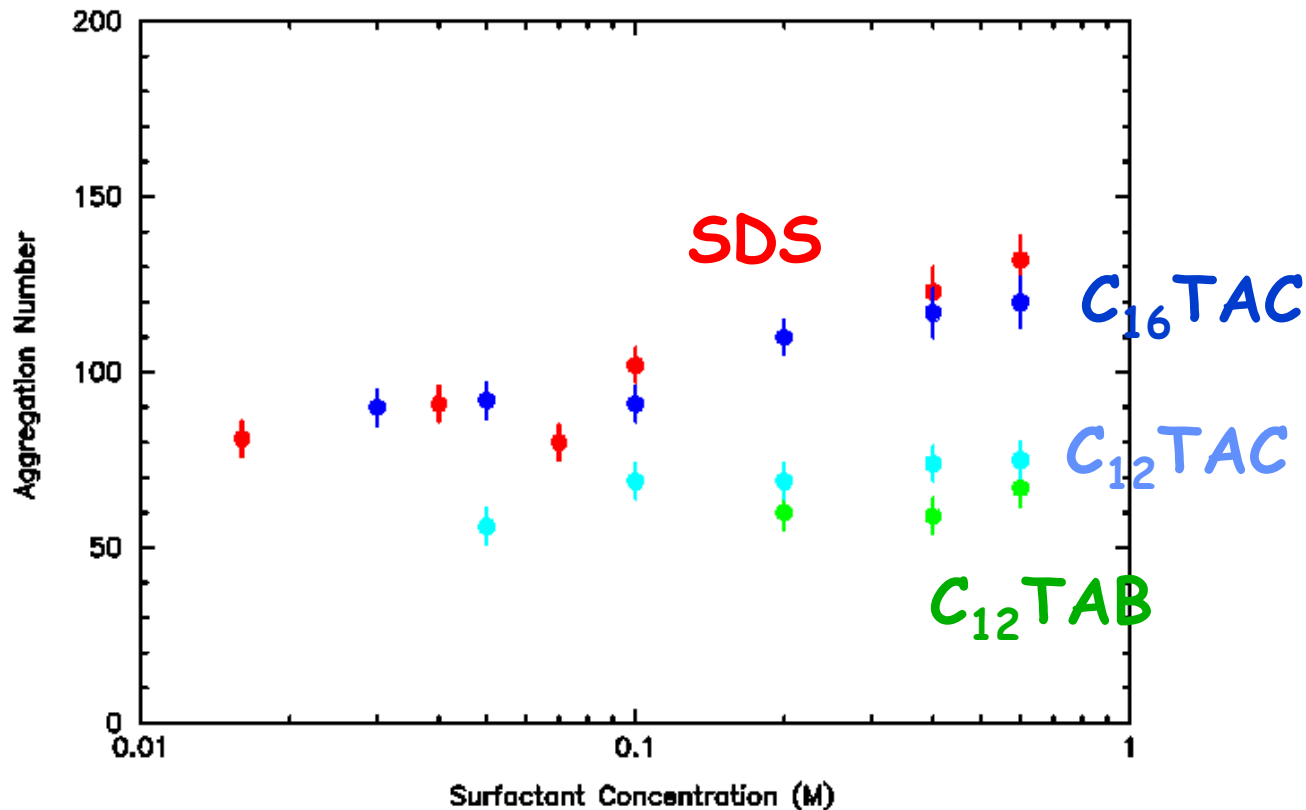
0.03M $C_{16}TAC$ in D_2O



0.6 and 1.2M Na Octanoate in D_2O



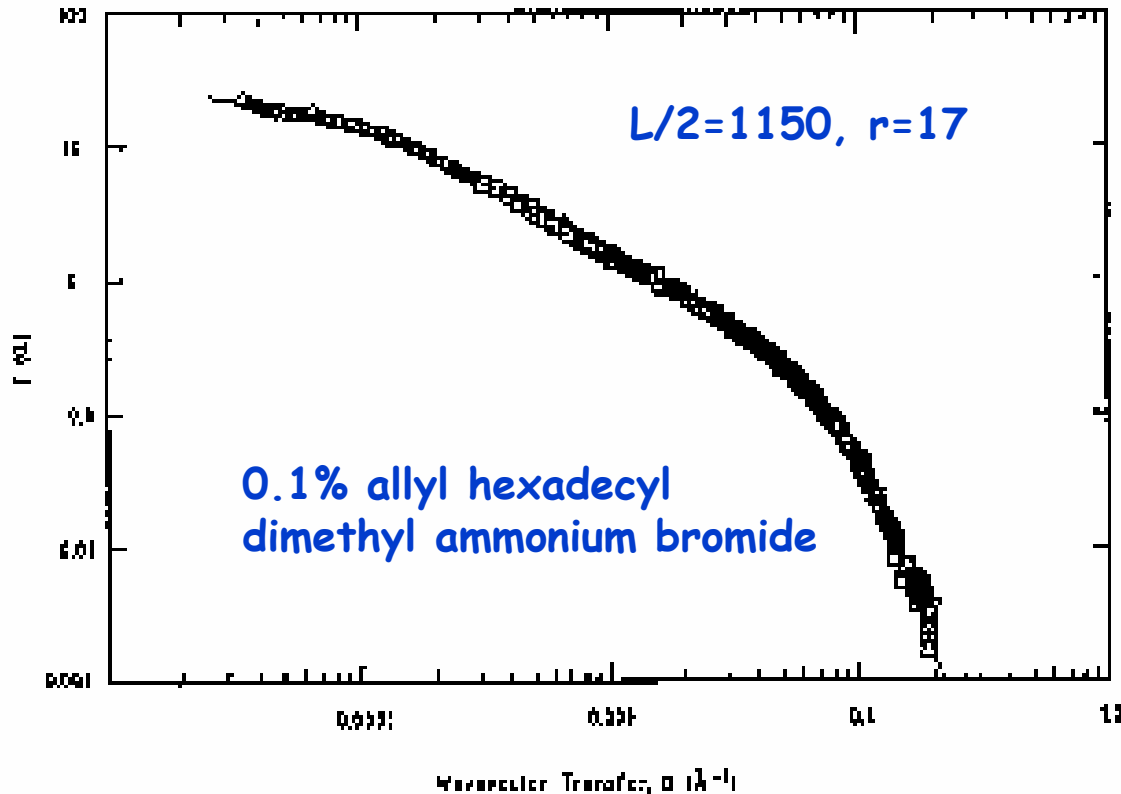
Some model parameters for some simple micelles



Effect of concentration

C₁₂TAB (C) : small spherical micelles
SDS, C₁₆TAC : elliptical, ee 1.23 to 2.47

Micelle Growth : elongated structures

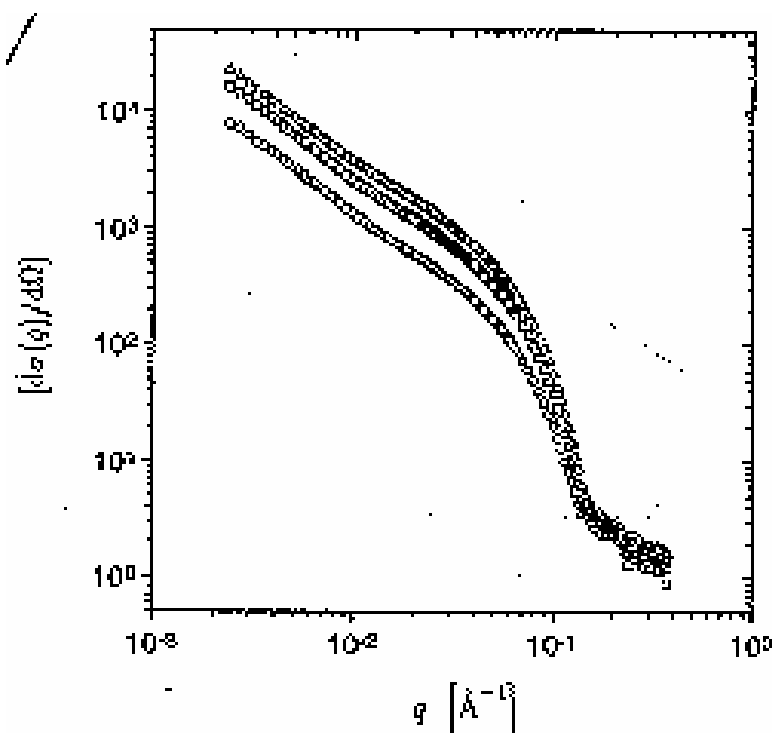


Surfactant conc, electrolyte
induces micellar growth to
rod-like structures

Counterions, such as salicylate,
induce extreme growth and
highly elongated structures

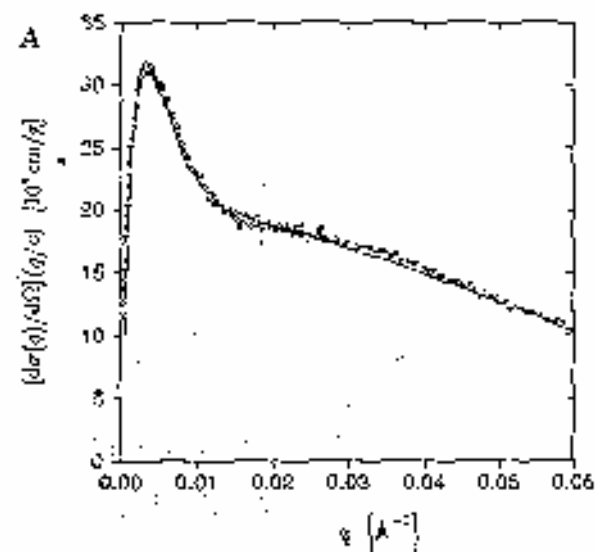
Measured over 3 decades of Q , and 4 decades of intensity
Consistent with randomly oriented rigid cylinders with
exponential distribution of lengths

Micelle Growth : elongated structures



Persistence length,
 $l_p = 1.9/Q^*$

C16E6 in D2O,
0.6, 1.2, 1.8 g/L



Holtzer plot ($QI(Q) \propto Q$)
emphasises Q^{-1} to Q^{-2}
transition to provide estimate of
Persistence length

C16E6 shows substantial conc induced growth of,
interpreted as polymer-like micelles or worm-like chains

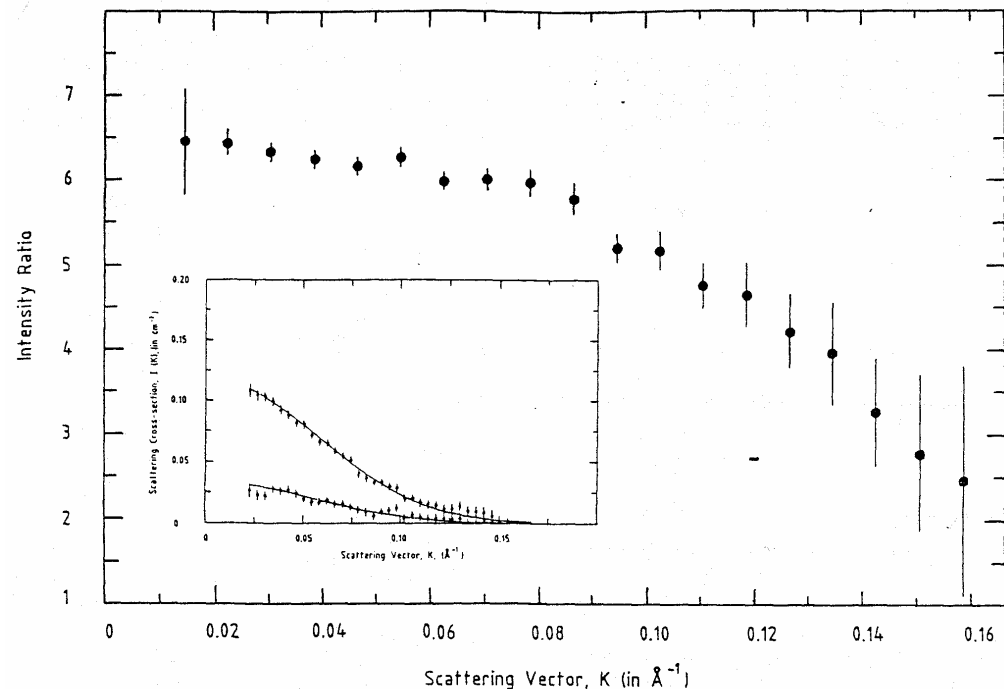
Composition of mixed surfactant micelles

If $P(Q)$, $S(Q) \sim 1.0$ then

$$I(Q) \approx \sum_i N_i V_i^2 (\rho_{ip} - \rho_s)^2$$

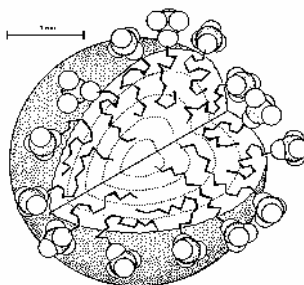
From measurements,
for example,
h-SDS/ h-C12E6 and
h-SDS / d-C12E6
in D2O

$$R = \frac{I(Q)_{hh}}{I(Q)_{hd}} (Q \rightarrow 0)$$

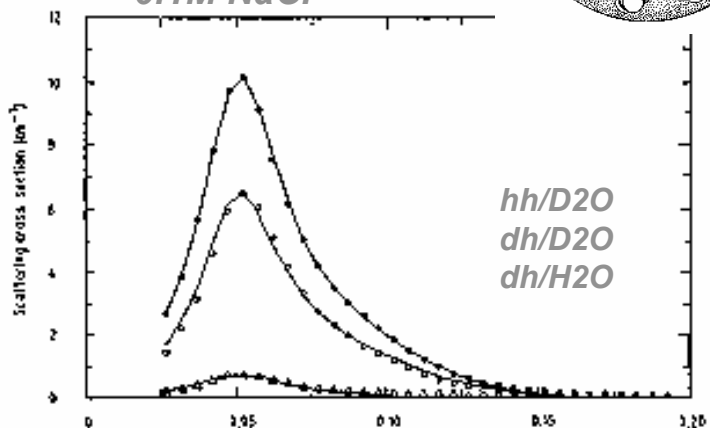


$$V_f = \frac{(\sqrt{R} - 1)(\rho_{hSDS} - \rho_{D2O})}{(\rho_{hC12E6} - \rho_{hSDS}) - \sqrt{R}(\rho_{dC12E6} - \rho_{hSDS})}$$

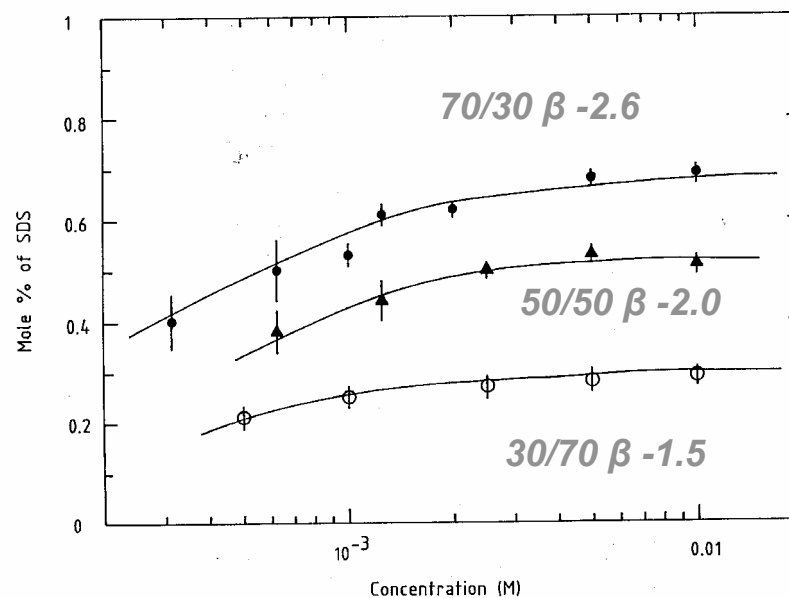
Mixed Surfactant micelles



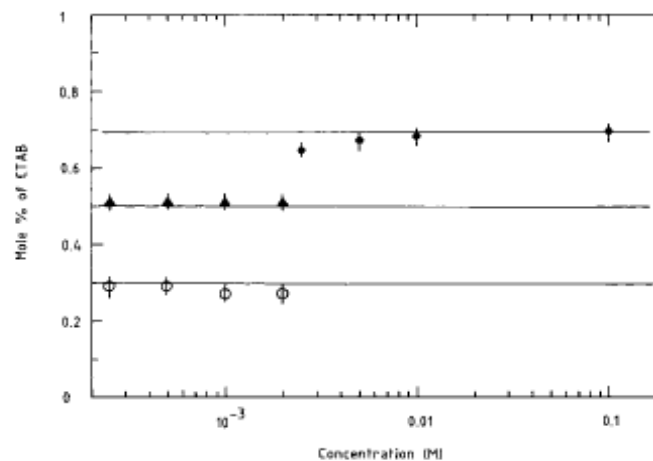
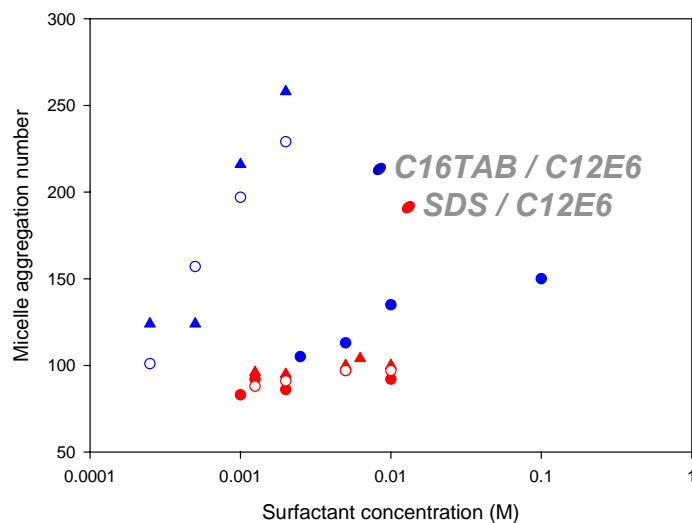
0.1 M C16TAB / C12E6
0.1M NaCl



SDS / C12E6 / 0.1M NaCl

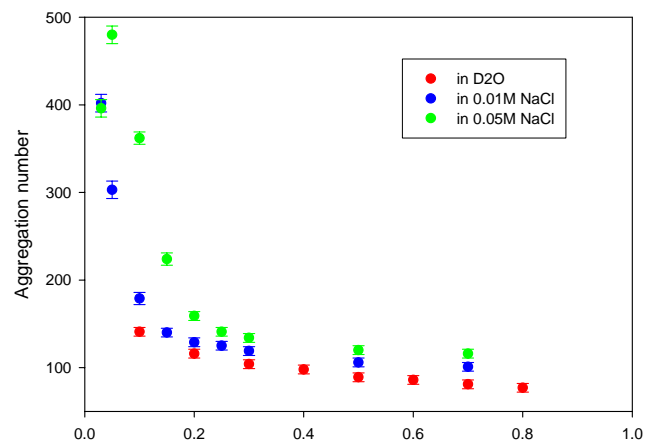


C16TAB / C12E6 0.1M NaCl



Mixed Surfactant micelles

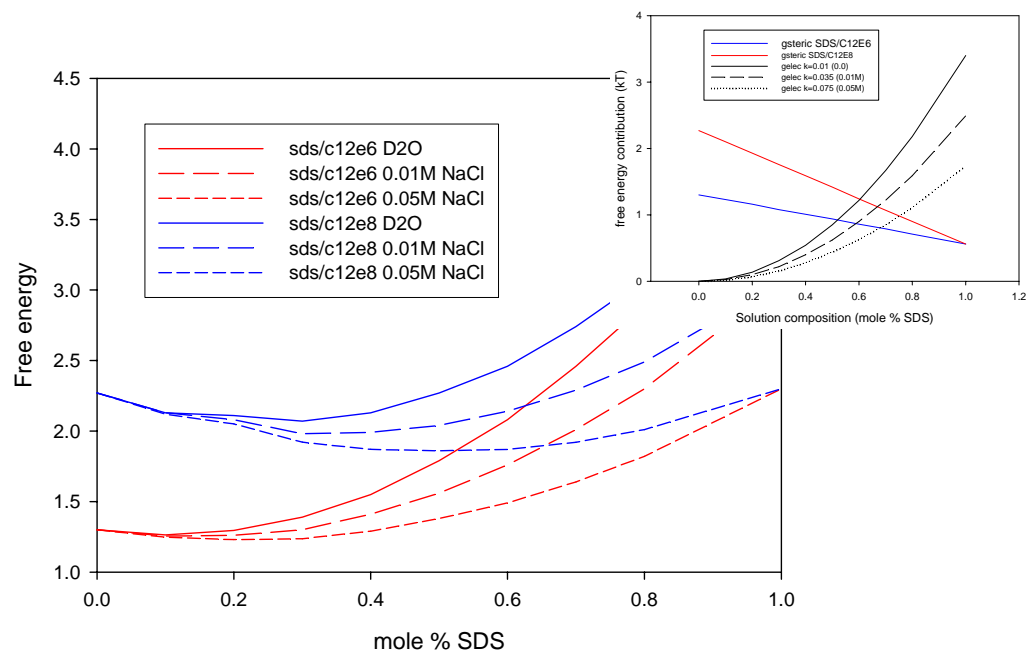
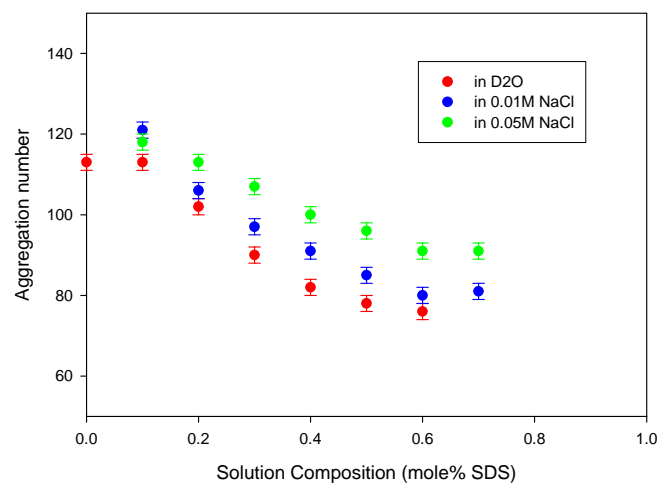
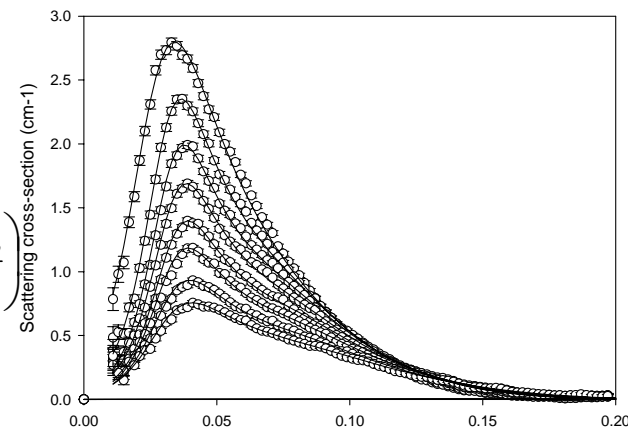
Simple free energy terms explains main trends
Growth of C12E6 rich micelles attributed to dehydration



$$v = \left(\frac{4\pi l_c^3}{3V_o} \right) \left(\frac{a_e l_c - 2}{V_o} \right)^{-1}$$

$$g_{ster}^{mix} = -k \left[\alpha \ln \left(1 - \frac{a_{ha}}{a} \right) + (1 - \alpha) \ln \left(1 - \frac{a_{hb}}{a} \right) \right]$$

$$g_{elec}^a = \frac{2\pi e^2 d}{\epsilon a_e} (1/1 + \kappa_o l_c)$$



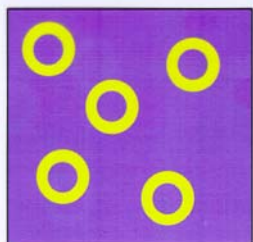
Alkyl chain contribution
~ -17 to 18 kT

Penfold et al, J Phys Chem B
109 (2005) 10760

More significant variation in headgroup
contribution for C12E6 than for C12E8

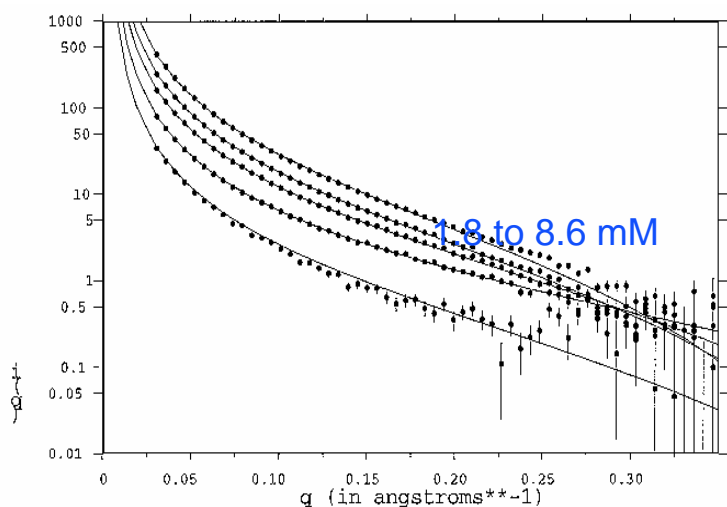


Adsorption of mixed surfactants (SDS / C12E6) at the oil-water interface



Prepare hexadecane in water emulsions($\sigma \sim 0.2$ microns)
by ultrasound

Use h/d hexadecane to index match
to D2O Can dilute and add surfactant

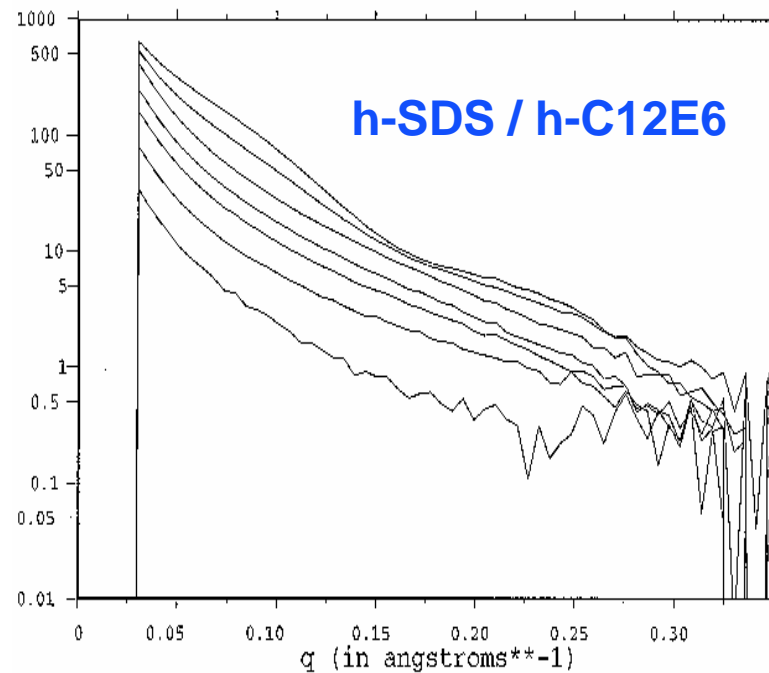


Adsorbed layer thickness varies
from 8 to 15 Å

Adsorbed amount from
 2.05 to 6.68×10^{-10} mol cm $^{-2}$



Penfold et al, J Phys Chem B 104 (2000) 606

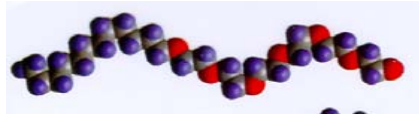


See Scattering from adsorbed
layer only + free micelles

Adsorbed amounts and composition from

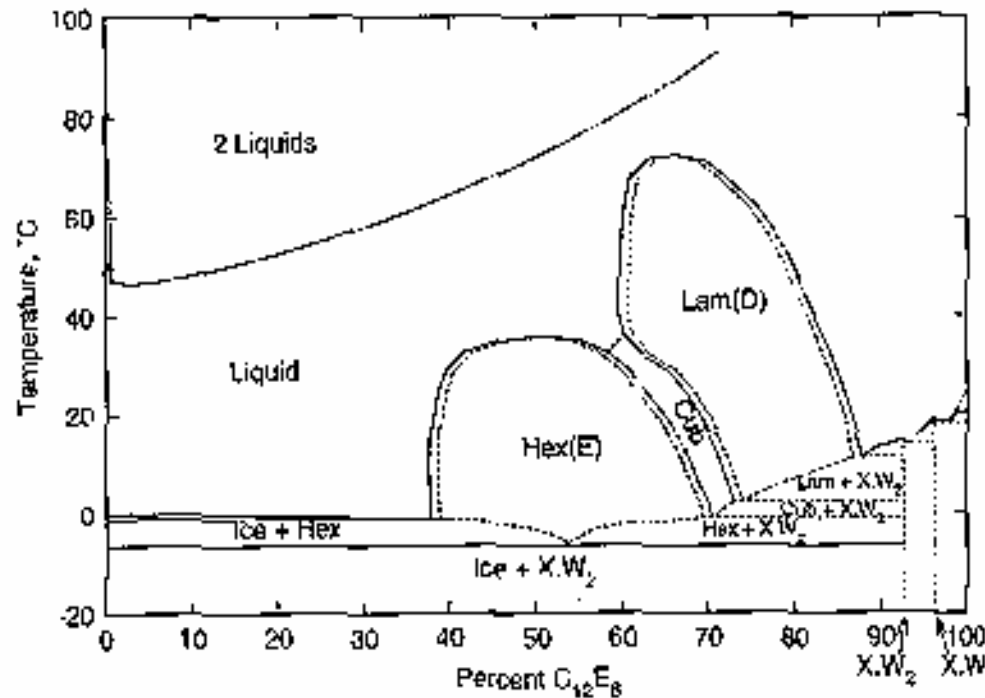
$$\Gamma = \frac{d(\rho_s - \rho_2)}{N_a V(\rho_s - \rho_a)}$$





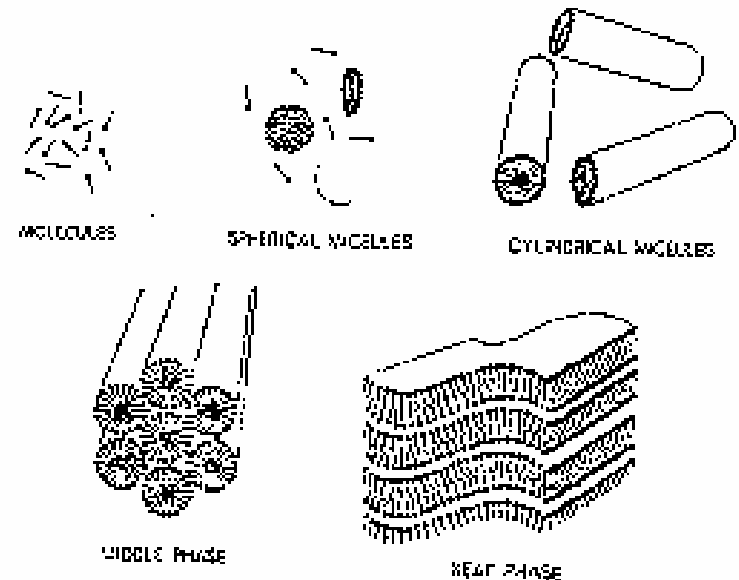
Conc / ordered Systems

Lyotropic micellar and liquid crystalline phases



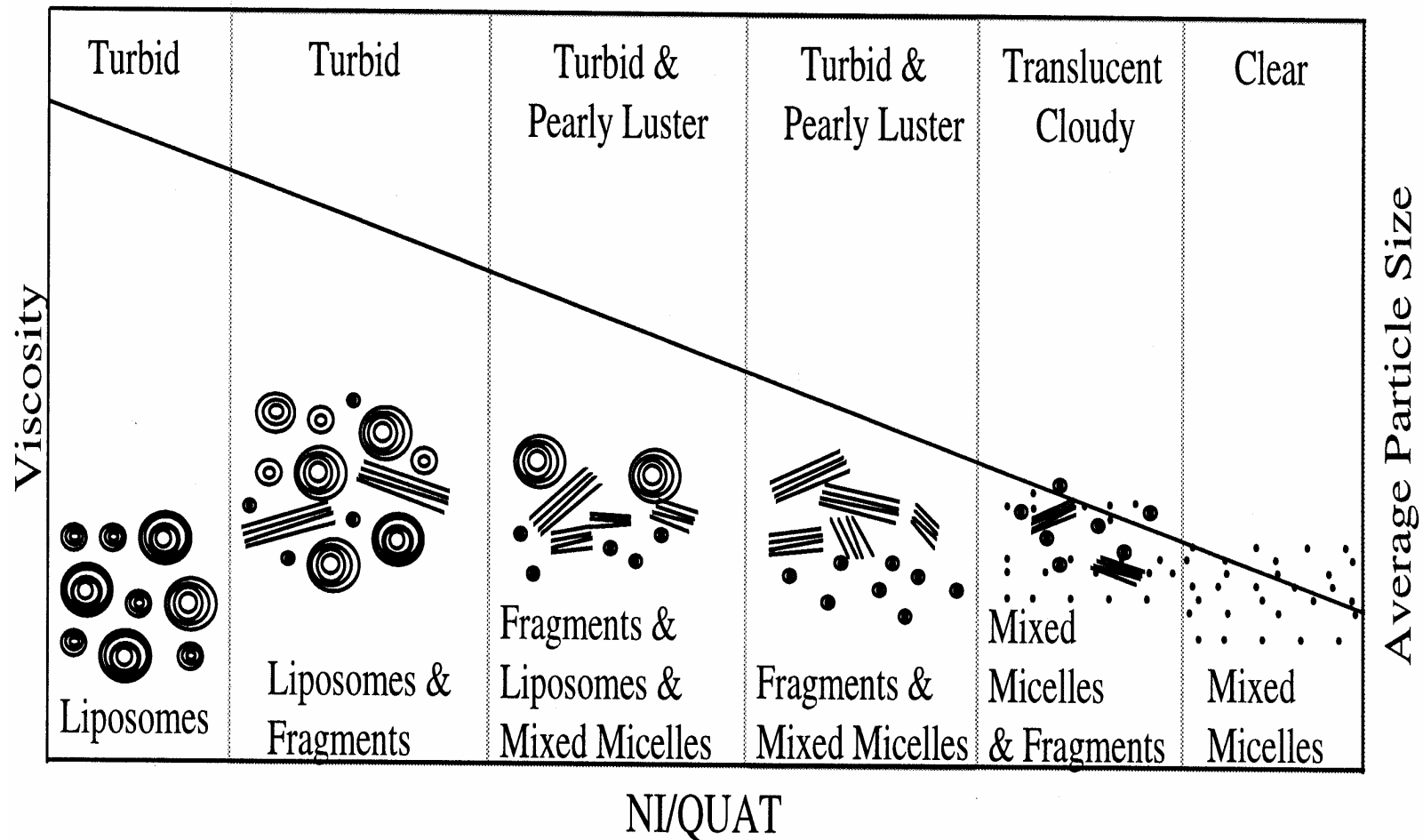
Phase diagram for C12E6

Progression of micellar shapes based on simple geometric constraints



$V/A \leq 1/3$	Spherical
$1/3 < V/A \leq 1/2$	Rods
$1/2 < V/A \leq 1$	Bilayers
$V/A > 1$	Inverted

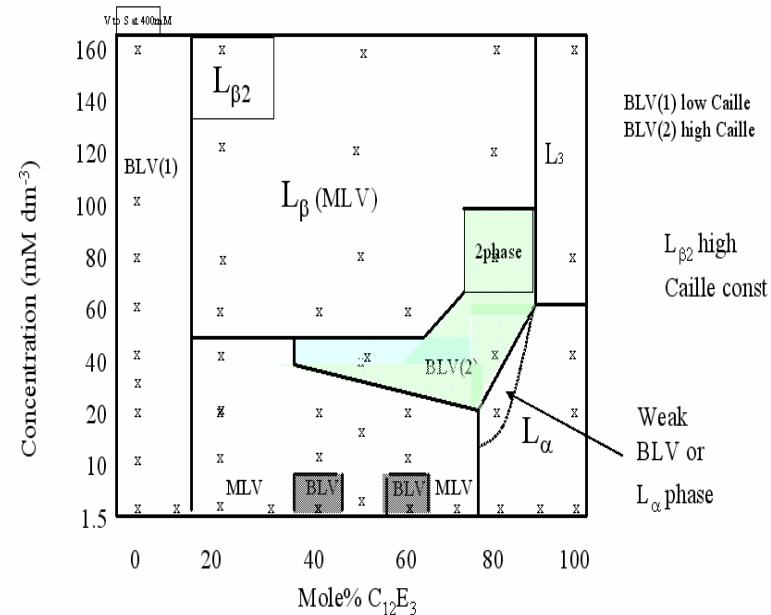
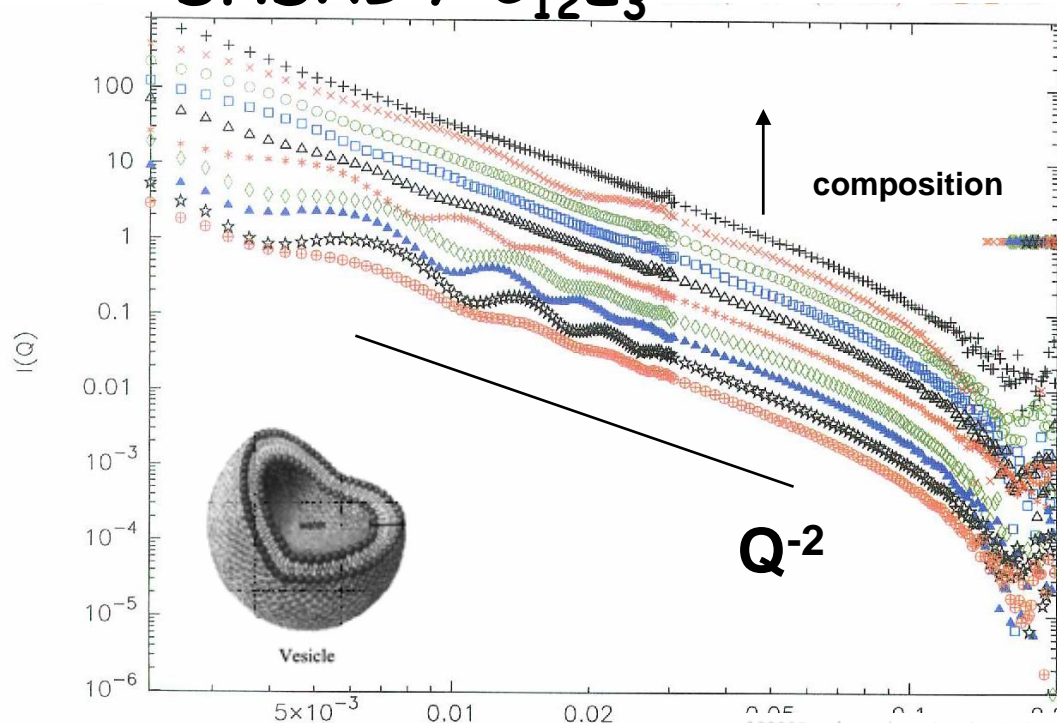
Increasing order with increasing surfactant concentration
Additional phases (not shown) include cubic, bicontinuous, mlv



Complex evolution of solution microstructure, from cationic to nonionic rich. Related to relative preferred curvature of the different surfactant components.

Now seen in a variety of different systems, which include lipid / nonionic mixtures and other ionic / nonionic surfactant mixtures

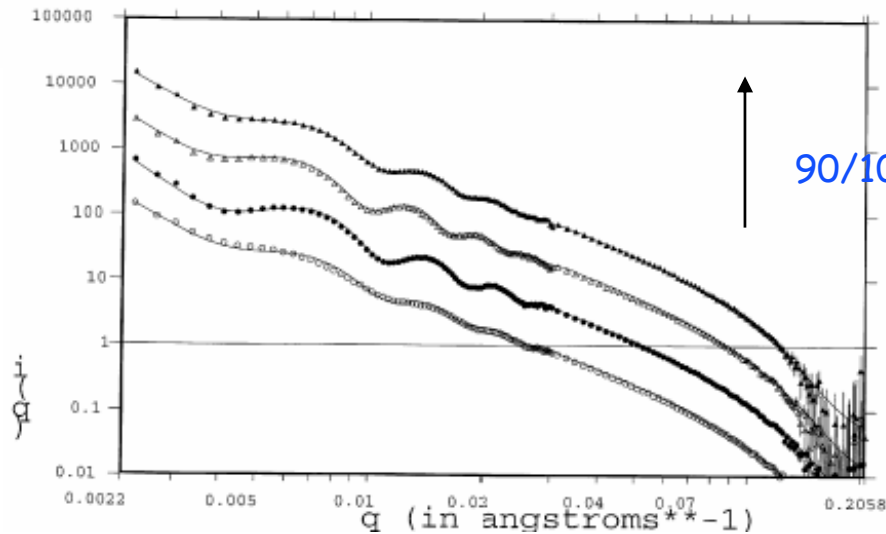
DHDAB / C₁₂E₃



1.5 mM DHDAB / C12E3
Bi-lamellar vesicles

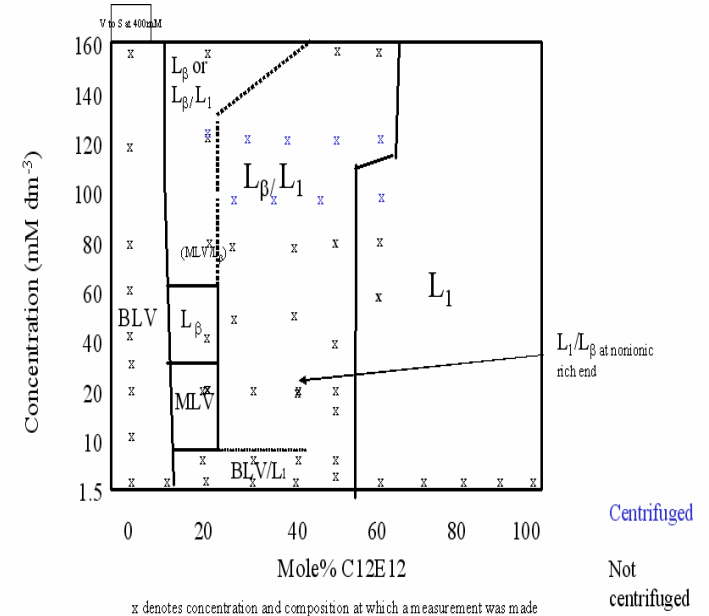
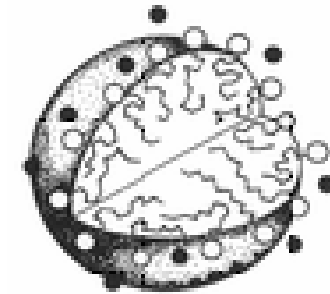
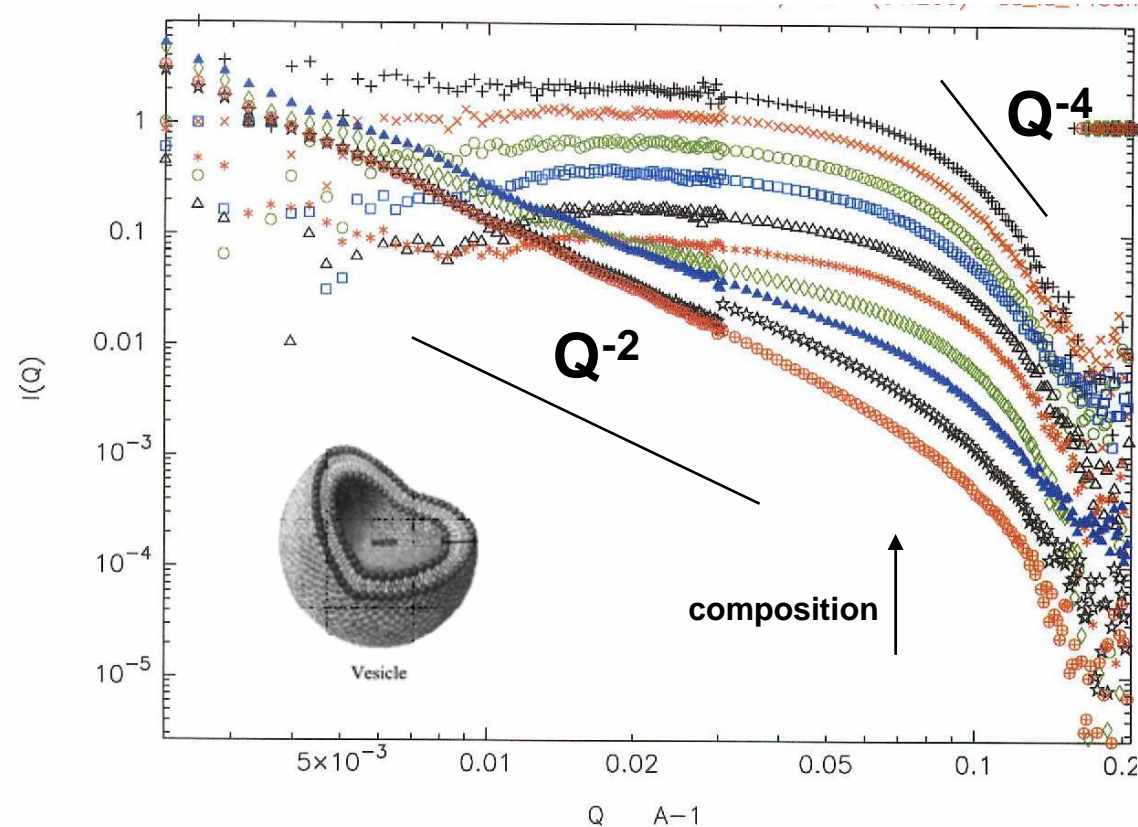
$$\eta = \frac{Q_0^2 k_B T}{8\pi \sqrt{\kappa B} / d}$$

$d \sim 850$ to 1150
 $\delta \sim 28$ to 32
 $\eta \sim 0.02$ to 0.05



ISIS

DHDAB / C₁₂E₁₂



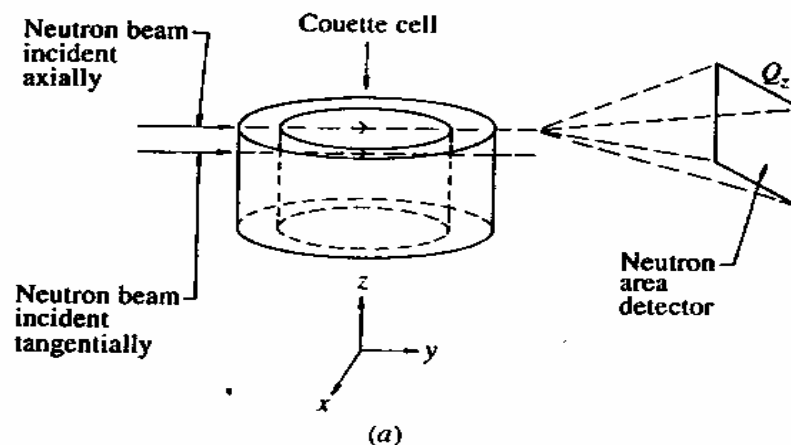
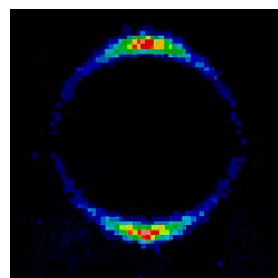
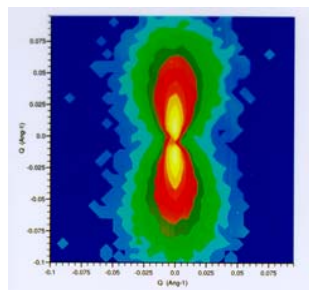
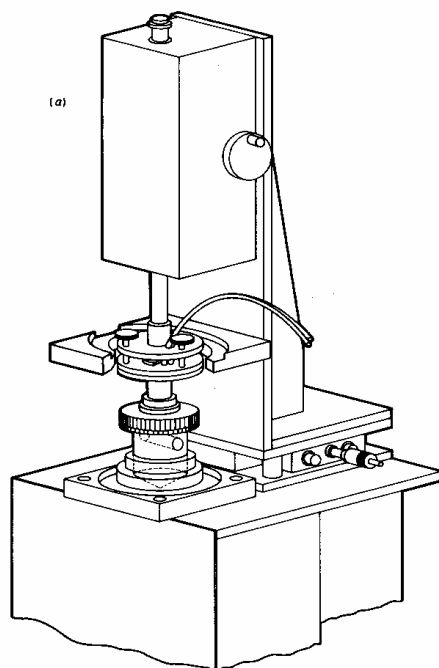
For nonionic rich, globular micelles which grow with increasing cationic content, extensive micellar region

At low concentrations, transition to vesicles
At higher concentrations, transition to L_β, and coexistence region

Penfold et al, Langmuir 20 (2004) 1269

Shear flow alignment / orientation

Couette Flow Cell



$d \ll r$ shear gradient constant across gap

For ISIS Couette cell 0.5mm $G=5.28N$

Outer cylinder rotates

G/Dr : Elongated particles, tend to align in flow direction, Brownian motion randomises alignment, Dr

Significant alignment when $G \gg Dr$

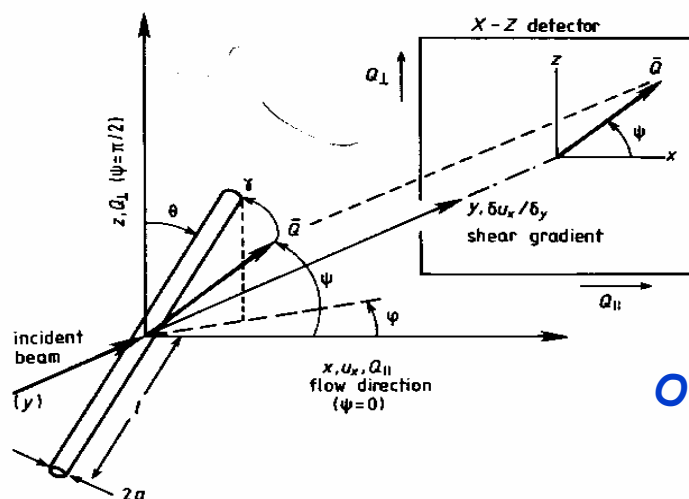


J B Hayter, J Penfold, J Phys Chem 88 (1984) 4589
H G Jerrard, Chem Rev 51 (1852) 345
H Thurn, J Kalus, H Hoffmann, J Chem Phys 80 (1984) 3440



For orientation in Couette flow,

$$I(Q) = I(Q, \Psi) = A \int_0^{2\pi} d\phi \int_0^\pi P(\theta, \phi; \Gamma) [F^2(Q, \gamma^+) + F^2(Q, \gamma^-)] \sin \theta d\theta$$



$$\cos \gamma^\pm = \sin \theta \cos \phi \cos \psi \pm \cos \theta \sin \psi$$

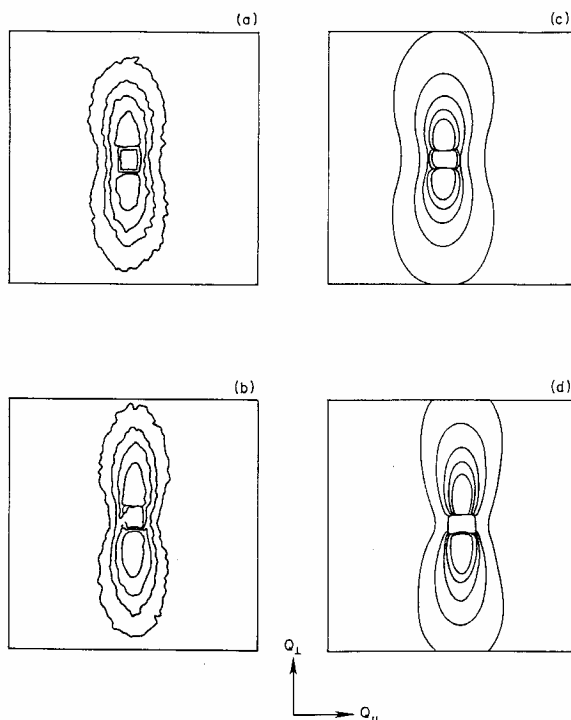
Q_\perp refers to $\Psi = 0$

Q_\parallel refers to $\Psi = \pi/2$

Orientation distribution comes from solution to the diffusion equation

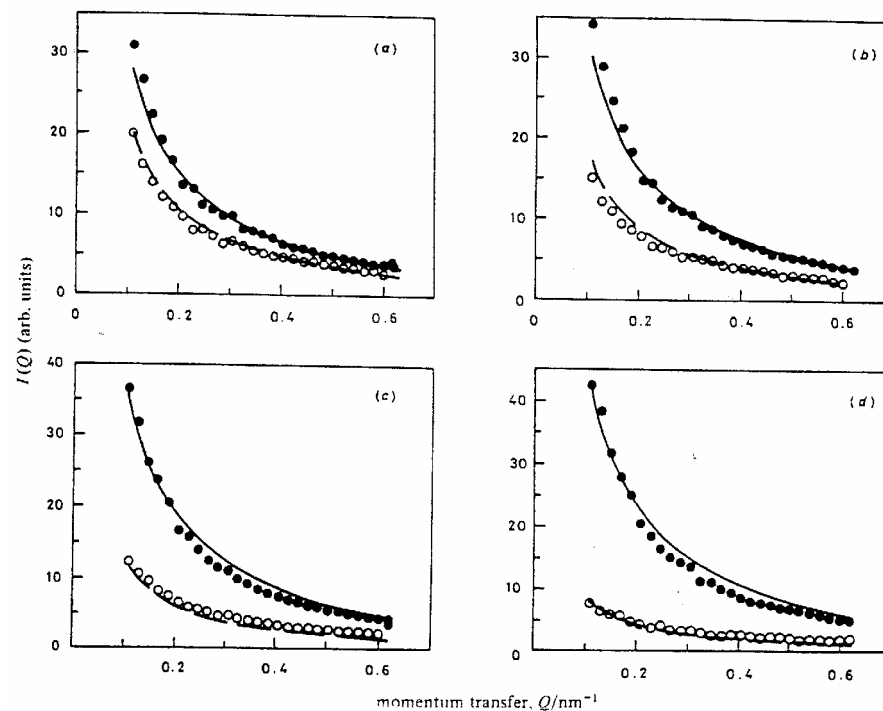
$$2\phi_0 = \arctan(8/\Gamma) \quad P(\theta, \phi; \Gamma) = \frac{(1 - \cos^2 \phi_0)(1 + \sin^2 \theta \cos 2\phi_0)^{3/2}}{4\pi(1 - \sin^2 \theta \cos 2\phi_0 \cos 2(\phi - \phi_0))^2}$$

Elongated Micelles (rod-like)



0.04M DDACl / 4M NaCl (a) $G=2000 \text{ s}^{-1}$ (b) 3000
(c) 5000 and (d) 7000

Calculation for $2l=2500$, $2a=44$



0.03M C16TAB / 0.4M KBr at
(a) $G=5000 \text{ s}^{-1}$ and (b) $G=7500 \text{ s}^{-1}$

Calculation for $2l=2700$, $2a=47$

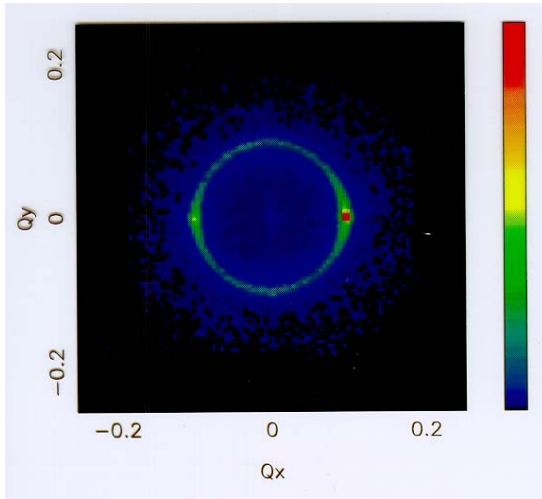
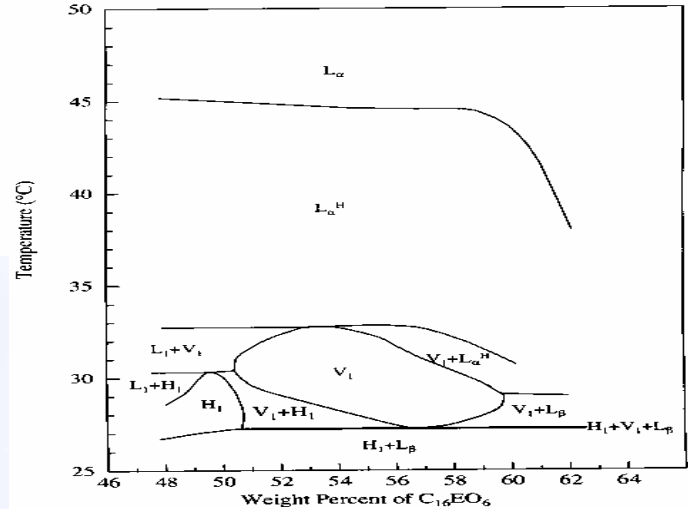


PG Cummins, E Staples, J Penfold, J B Hayter, J Chem Soc Farad Trans 83
(1987) 2773, Langmuir 5 (1989) 1195, Chem Phys Lett 138 (1987) 436

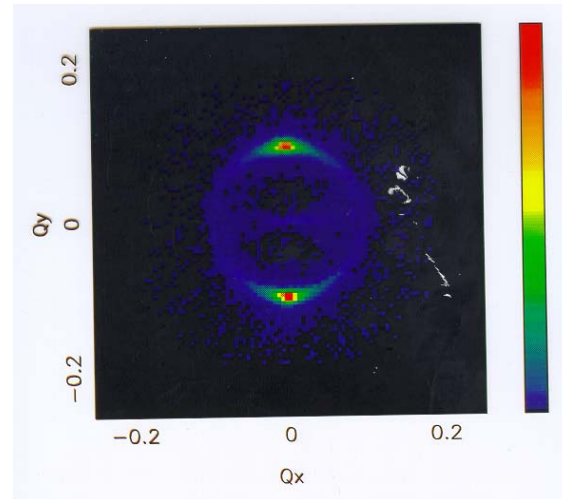


Orientational order in concentrated lamellar phases

51 wt % C16E6

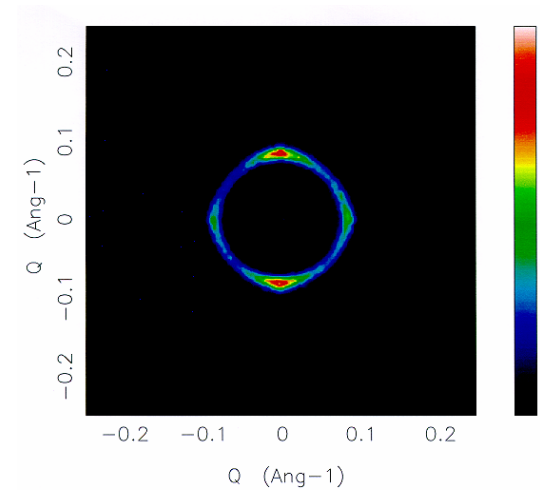


Cell side, low shear



Cell centre, $G=5000s^{-1}$

Aligned parallel to flow-vorticity plane at low shear,
and parallel to flow-shear gradient plane at high shear



At intermediate shear see
more complex distribution

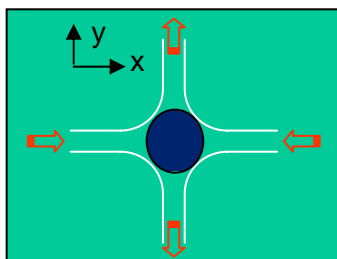


(Penfold, Staples, Khan Lohdi, Tiddy, Tucker,
J Phys Chem 1997 101 66)

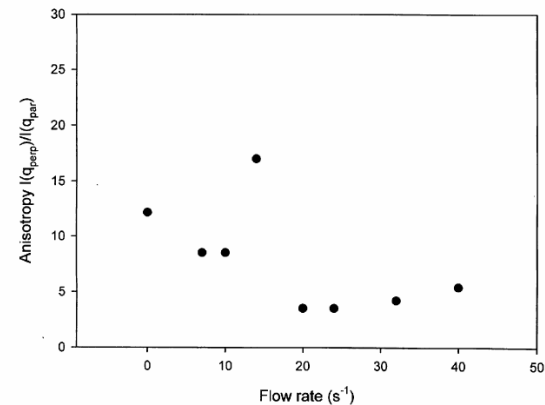
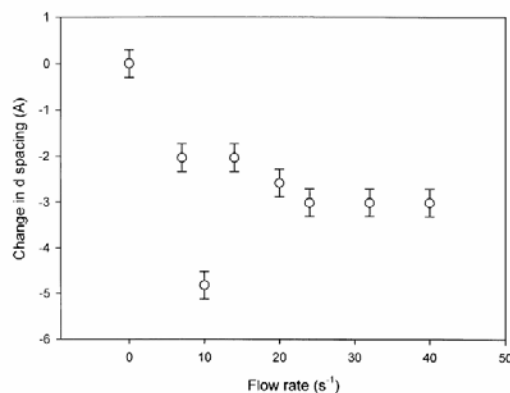
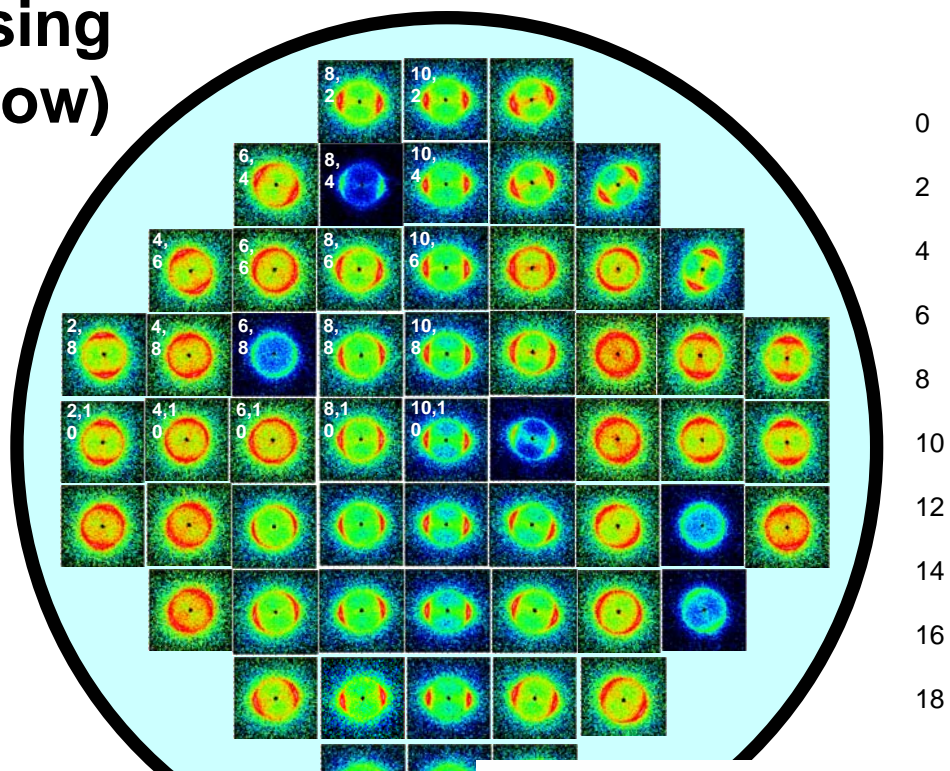
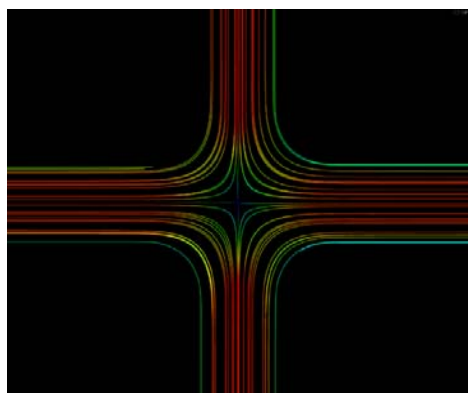


Mapping flow fields using SANS (elongational flow)

50.6 wt% C₁₆E₆ / D₂O at 55°C
Lamellar phase dispersion



Distribution of orientational order reflects flow pattern

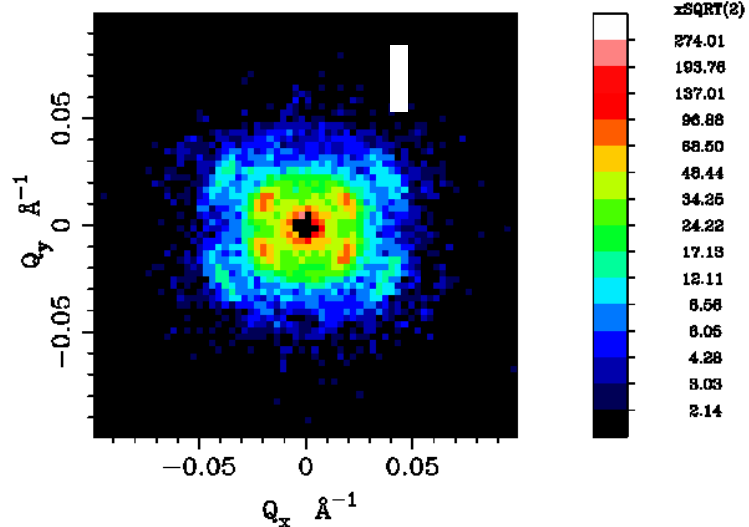
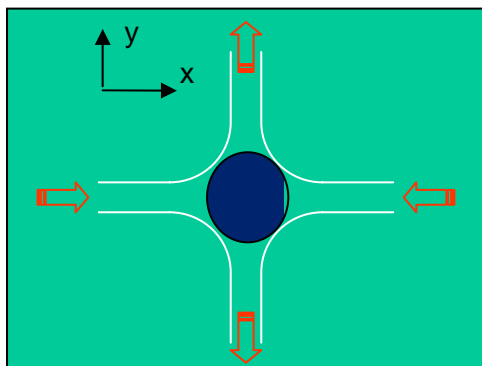


In anisotropy and d spacing variation with flow rate, see stretching of lamellae sheets and reduction in domain size

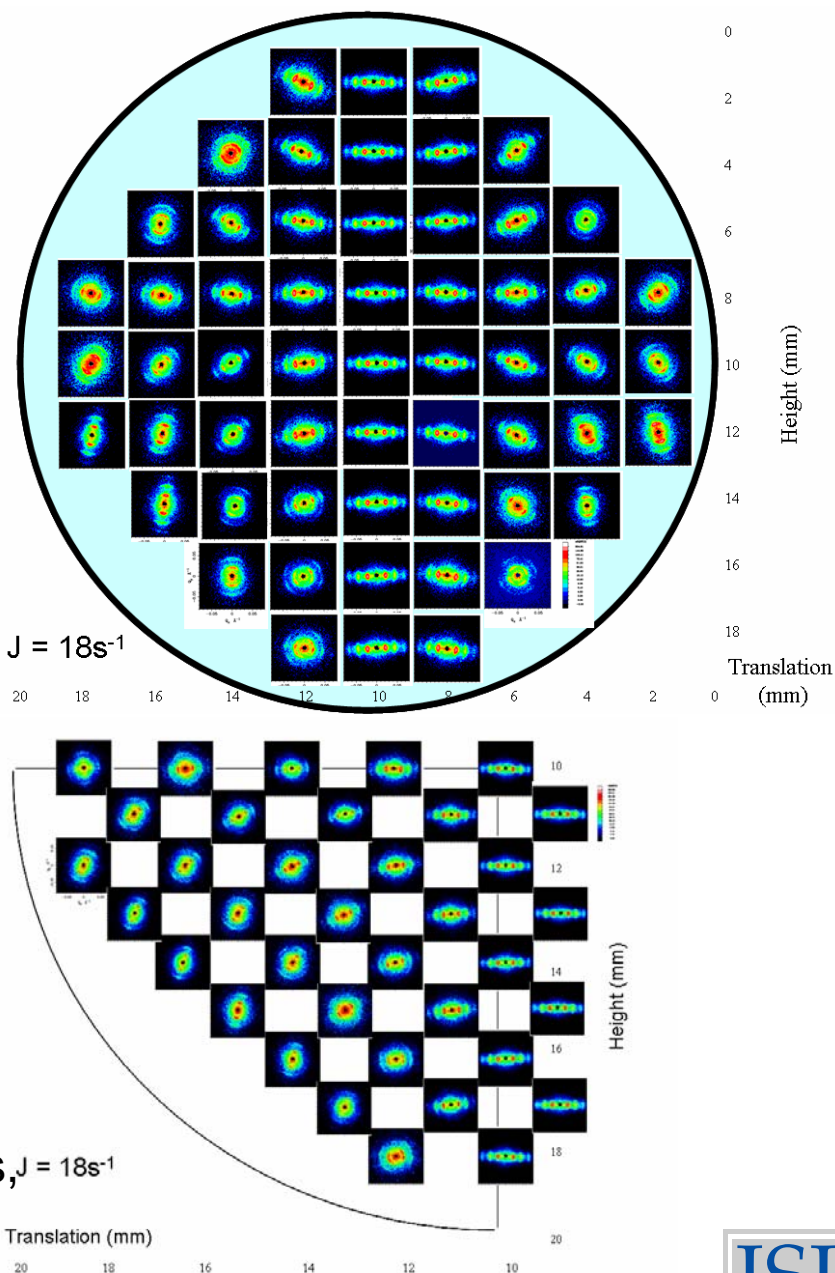
J Penfold et al, J Phys Chem B 110 (2006) 1073



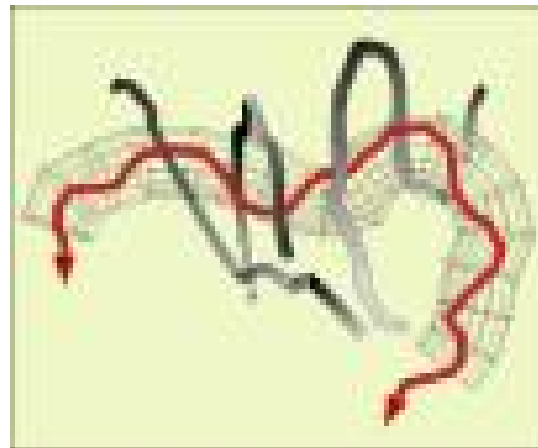
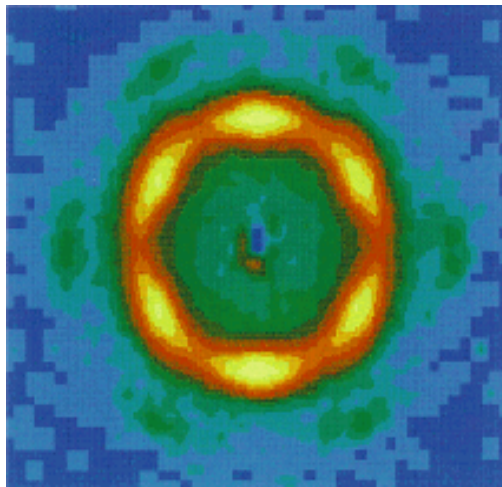
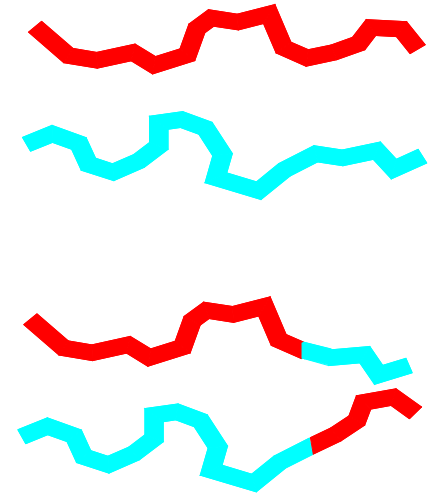
Flow induced effects in mixed surfactant mesophases



De-mixing in principle flow directions, $J = 18\text{s}^{-1}$
form of 'banding'



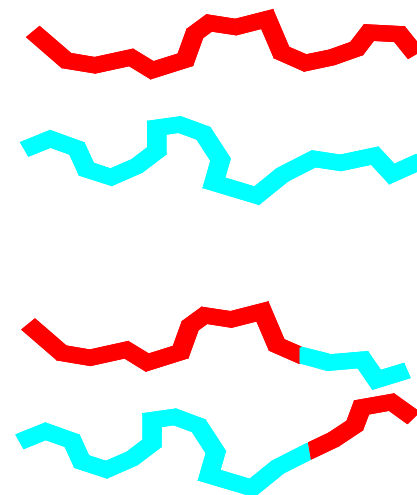
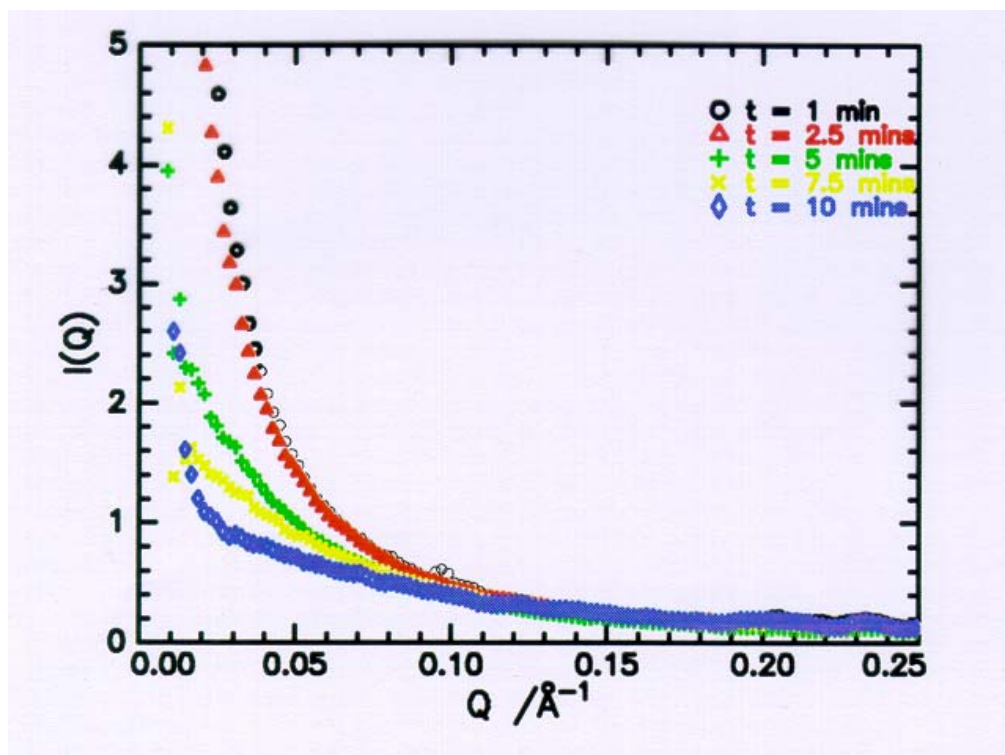
Polymers and polymeric materials



Kinetics of co-polymer trans-esterification

(Backsona, Richards, King, Polymer 40 (1999) 4205)

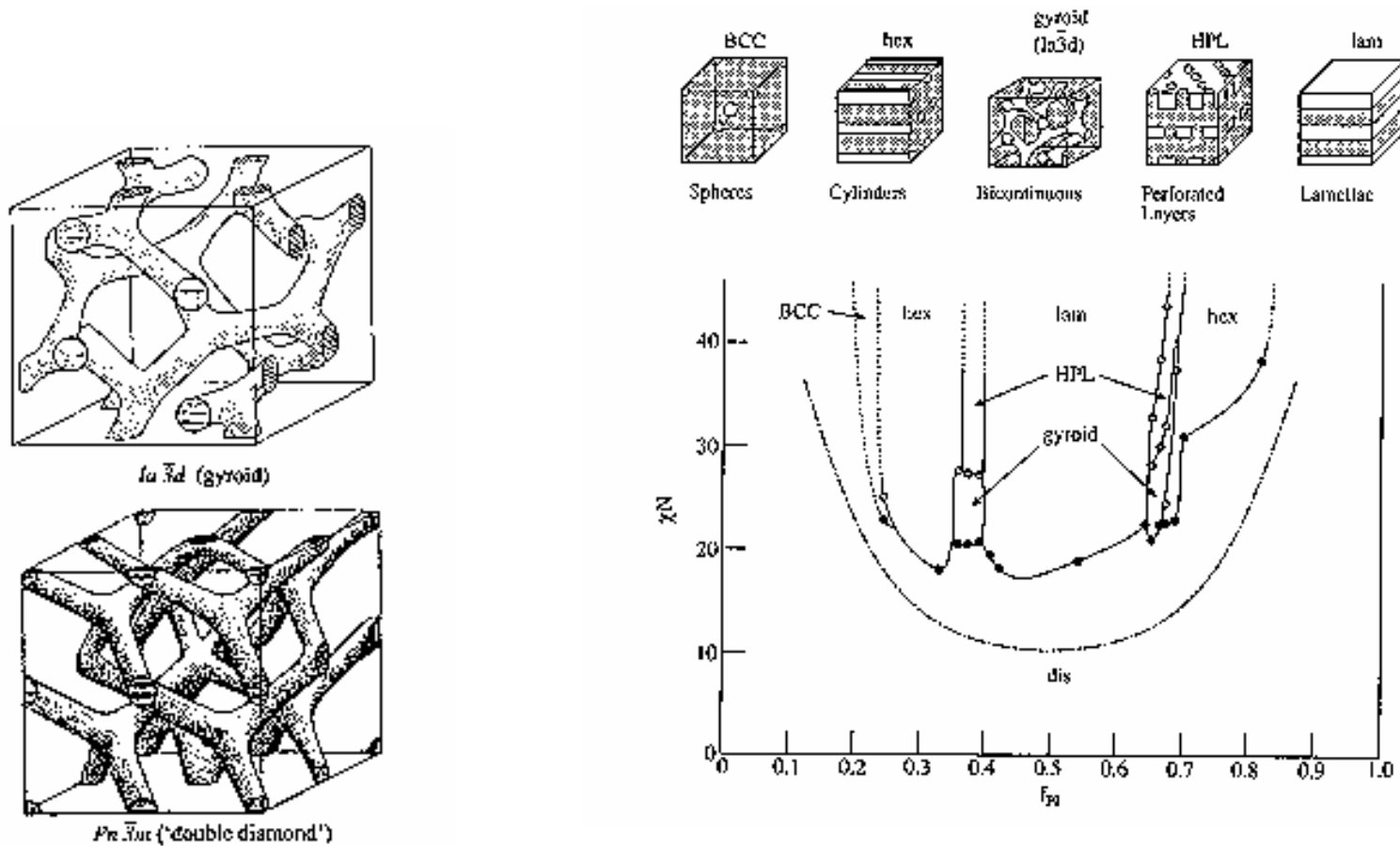
Polyesters, such as PET (polyethylene terphalate)
extensively used in packaging
PEN (poly-ethylene napthalene 2 6 dicarboxylate) has
superior physical properties but due to high processing
costs wish to use as blend



At elevated temperatures
interchange reactions (scission
and recombination),
TRANS-ESTERFICATION,
occurs

Follow reaction kinetics
in-situ using SANS

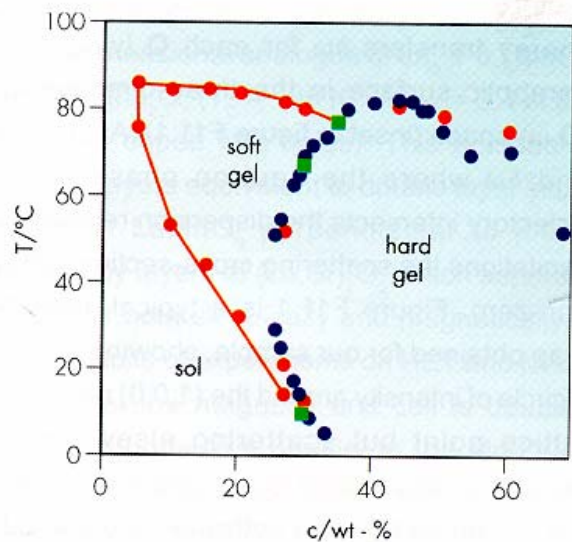
Block co-polymer ordered phases



Poly-styrene - poly-isoprene
block co-polymers

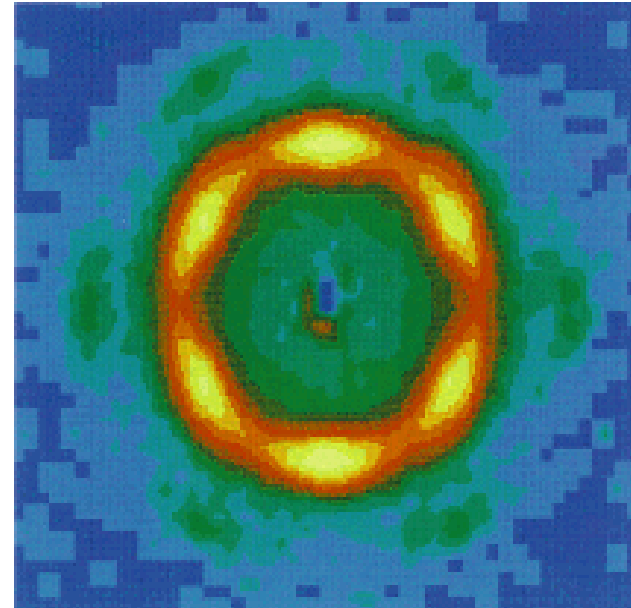
Microstructure of aqueous gels (block copolymers)

Phase diagram of aqueous solutions of E41B8 (oxyethylene-oxybutylene block copolymer) forms micellar gel with cubic packing
Hard gel is bcc or fcc, depending on preparation conditions, soft gel is a defective cubic phase



Oriented fcc gel, induced by shear flow

Shear \rightarrow



SANS from fcc gel of 25% E41B8 in 0.1M K2SO4 (oriented under shear)



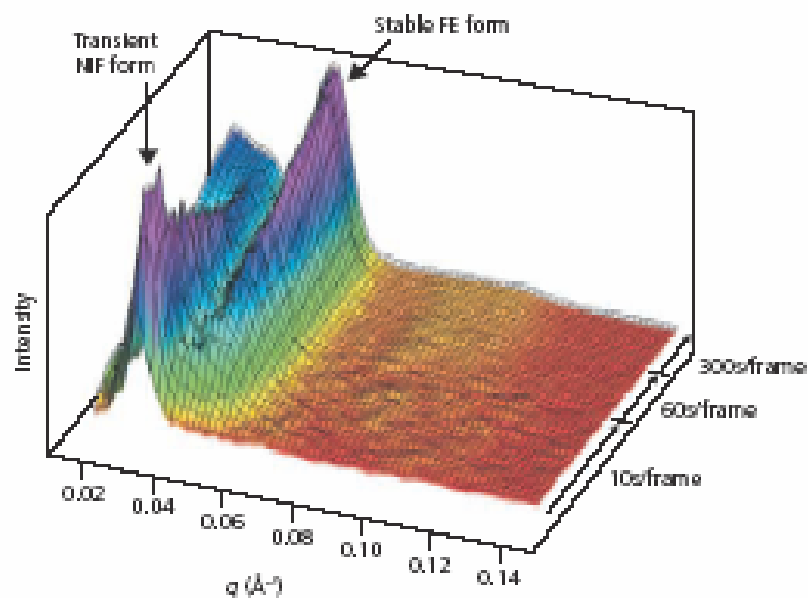
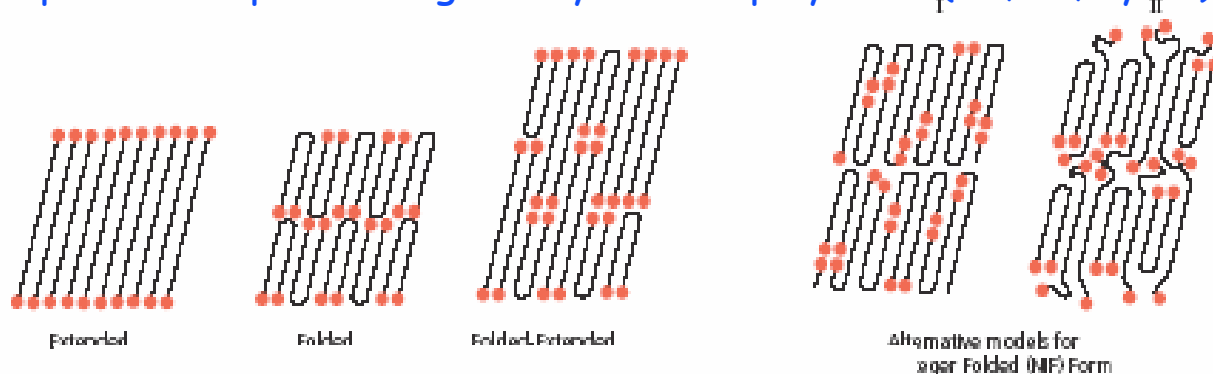
Phase diagram of aqueous solution of E41B8

C Booth, G E Lu, S M Mai, B U Komaneschek, S M King, I A Hamley, J A Pople, A J Ryan, J P A Fairclough, N J Terrill



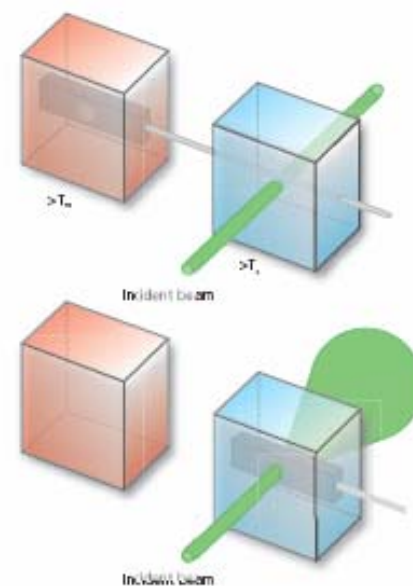
Real time SANS study of transient phases in polymer crystallisation (Ungar, Spells)

Polymers often crystallise through transient phases, Important in processing of crystalline polymers (PE, PP, nylon)



SANS data show that initial transient structure is in form of NIF which subsequently transforms to FE.

Final structures can be E, F, or FE



Structural rearrangements in polymer / surfactant mixtures (Cosgrove et al)

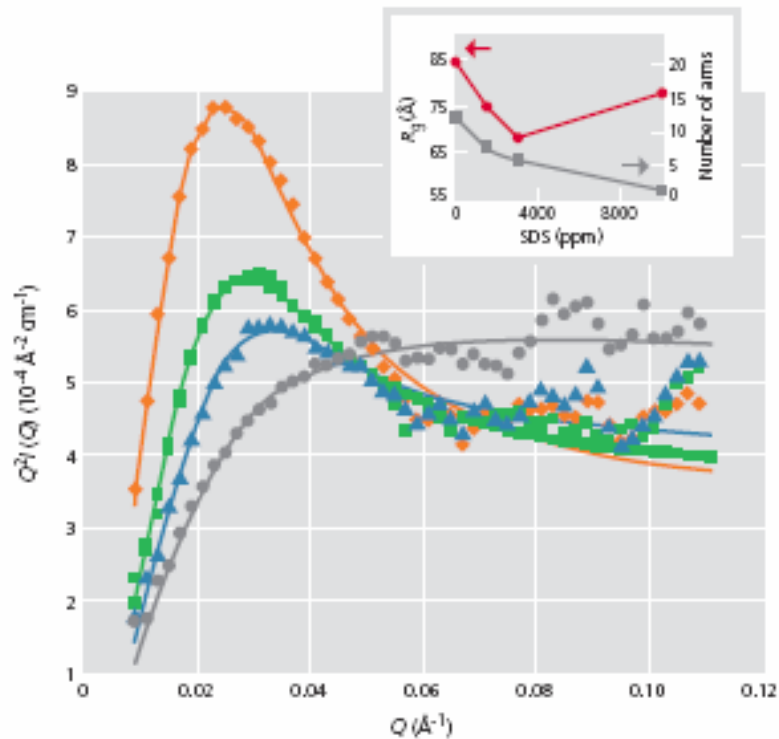
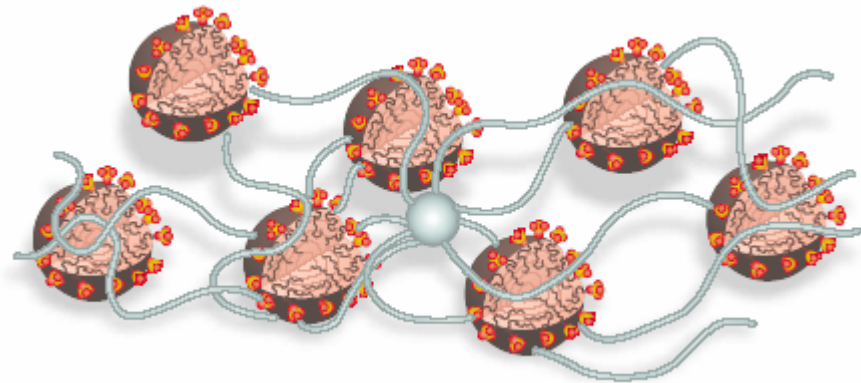


Fig. 1: SANS data shown as $Q^2 I(Q)$ against Q , for 15-arm PEO star ($130000 \text{ g mol}^{-1}$) in D_2O , adding D-SDS.
 ♦, without SDS; ■, 1500 ppm SDS; ▲, 3000 ppm SDS; ●, 10000 ppm SDS. Solid lines are fits to the Benoit star form factor, with the corresponding radius of gyration and the number of arms shown in the inset.

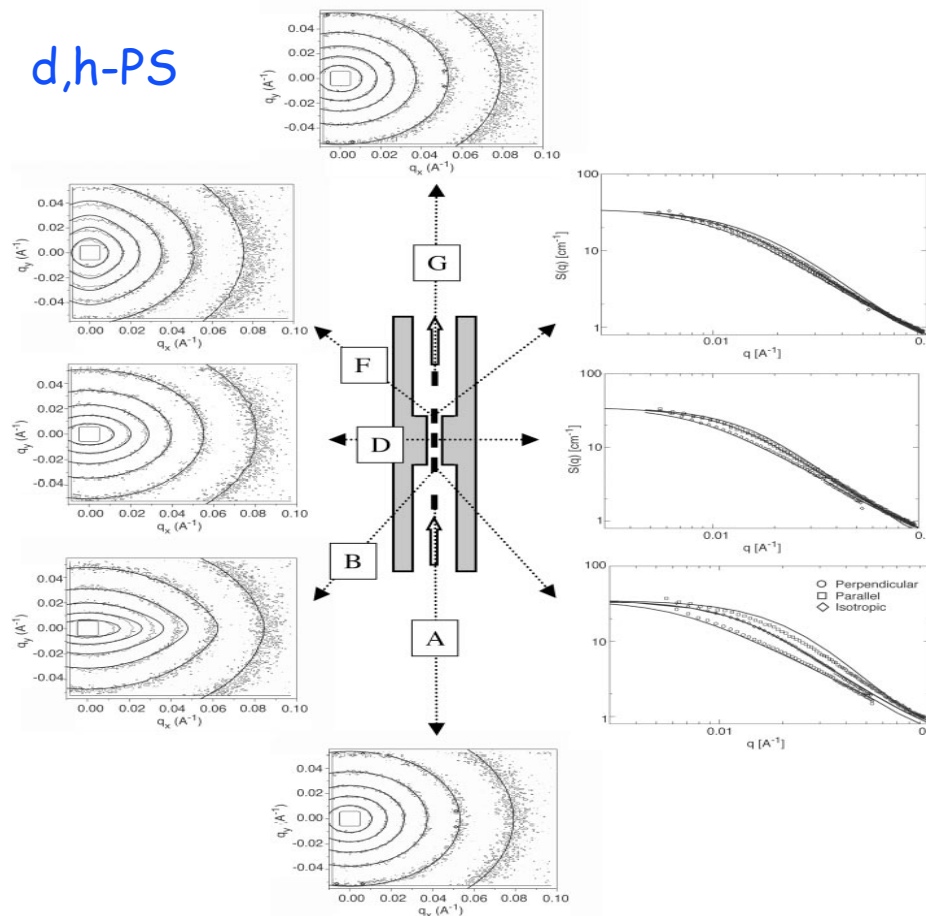
Weakly interacting polymer
chains / surfactants
form 'pearl necklace' structures



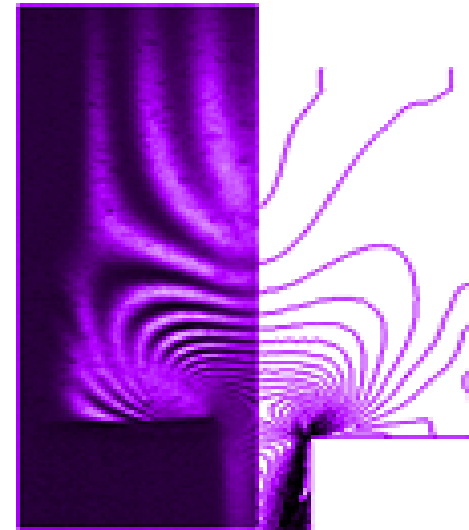
Rather different behaviour
seen when polymer is in form
of star rather than linear chain

Binding of micelles to arms of
star forces conformational
transformation into
two bundles of stretched arms

Mapping polymer flow by SANS (McLeish et al)



Entangled polymer melt flow through extended contraction visualised by SANS



Comparison of birefringence (stress difference pattern), and theory

SANS and stress patterns calculated from 'tube' model
 Reptation + contour length fluctuations (tube breathing modes)
 + (in stronger flows) convective constraint release (disappearance / reappearance of entanglements due to flow)

Summary

Described basics of technique

Illustrated the scope of the technique with examples from Soft Matter, over a broad range that included,

Surfactant aggregates, emulsions, super-critical fluids, liquid crystalline phases, micro-gels, and polymers

Presented work from a number of collaborations and other groups, which include,

Richardson (Bristol), Ryan (Sheffield), Thomas (Oxford), Richards (Durham), Cosgrove (Bristol), Ungar (Sheffield), McLeish (Leeds), and Unilever